

Need Plates # 1-11-111



**EARTH SCIENCE LABORATORY  
420 CHIPETA WAY, SUITE 120  
SALT LAKE CITY, UTAH 84108  
TELEPHONE 801-581-5283**

TECHNICAL REPORT  
GEOTHERMAL POTENTIAL OF ASCENSION ISLAND, SOUTH ATLANTIC  
PHASE I - PRELIMINARY EXAMINATION

Prepared For

United States Air Force  
Eastern Space and Missile Center  
Patrick Air Force Base, Florida 32925

and

United States Department of Energy  
Idaho Falls Operations Office  
Idaho Falls, Idaho

By

Earth Science Laboratory  
University of Utah Research Institute

Dennis L. Nielson  
Bruce S. Sibbett

November 5, 1982

## NOTICE

This report was prepared to document work sponsored by the United States Government. Neither the United States nor its agent, the United States Department of Energy, nor any Federal employees, nor any of their contractors, subcontractors or their employees, makes any warranty, express or implied, or assumes any legal liability or responsibility for the accuracy, completeness, or usefulness of any information, apparatus, product or process disclosed, or represents that its use would not infringe privately owned rights.

## NOTICE

Reference to a company or product name does not imply approval or recommendation of the product by the University of Utah Research Institute or the U.S. Department of Energy to the exclusion of others that may be suitable.

## CONTENTS

	<u>Page</u>
1.0 EXECUTIVE SUMMARY.....	1
2.0 INTRODUCTION.....	3
3.0 GEOLOGY OF ASCENSION ISLAND.....	5
3.1 Regional Setting.....	5
3.2 Island Development.....	5
3.3 Island Geology.....	15
3.3.1 Introduction.....	15
3.3.2 Basalts.....	18
3.3.3 Andesites.....	30
3.3.4 Dacites and rhyolites.....	30
3.3.5 Xenoliths.....	38
3.3.6 Sediments and sedimentary rocks.....	39
3.3.7 Structural geology.....	39
3.3.7.1 Vents, explosion and subsidence features.....	40
3.3.7.2 Faults and structural trends.....	42
3.3.8 Thoughts on the eruption history of central and eastern Ascension Island.....	43
3.3.9 Alteration.....	46
3.3.10 Hydrology.....	46
3.3.11 Geochronology.....	49
4.0 GEOCHEMICAL SURVEYS.....	55
4.1 Introduction.....	55
4.2 Radon and mercury survey results.....	56
5.0 PHASE I CONCLUSIONS.....	62
6.0 PHASE II EXPLORATION STRATEGY.....	63
7.0 VOLCANIC HAZARDS.....	66
8.0 ACKNOWLEDGEMENTS.....	68
9.0 REFERENCES CITED AND ASCENSION BIBLIOGRAPHY.....	69
10.0 APPENDIX - PETROGRAPHIC DESCRIPTIONS.....	73

## FIGURES

	<u>Page</u>
Figure 3-1 Location of Ascension Island, the Mid-Atlantic Ridge and ocean fracture zones.....	6
3-2 Conceptual model for the development of Ascension island.....	8
3-3 Secondary mineral zonation in the IRDP hole.....	11
3-4 Thermal conductivity as a function of depth for basalt flows in the IRDP hole.....	13
3-5 Thermal conductivity as a function of depth for basaltic hypabyssal intrusives in the IRDP hole.....	13
3-6 Variation with depth of natural remnance, initial susceptibility, Konigsberger ratio and net magnetization for the IRDP hole.....	14
3-7 Classification of andesite, dacite, and rhyolite by $K_2O$ and $SiO_2$ contents.....	17
3-8 Total alkali-silica diagram for rocks of Ascension Island.....	19
3-9 AFM diagram of rocks from Ascension Island.....	20
3-10 Distribution of most recent flows on Ascension Island.....	23
3-11 Major structural zones on Ascension Island.....	41
3-12 K-Ar dates of three felsic units from Ascension Island.....	54
4-1 Radon and mercury survey results for AI-Sis survey.....	58
4-2 Radon and mercury survey results for AI-Pumice survey.....	58
4-3 Radon and mercury survey results for AI-Donkey survey.....	59
6-1 Phase II exploration strategy.....	64

## TABLES

	<u>Page</u>
Table 3-1 Whole-rock chemical analyses of basalts from flows around Sisters Peak and South Gannet Hill.....	24
3-2 CIPW norms of basalts from flows around Sisters Peak and South Gannet Hill.....	25
3-3 Whole-rock chemical analyses of other basalt flows from Ascension Island.....	27
3-4 CIPW norms of basalts from Ascension Island.....	29
3-5 Whole-rock chemical analyses of andesites from Ascension Island.....	31
3-6 CIPW norms of andesites from Ascension Island.....	32
3-7 Whole-rock chemical analyses of dacites and rhyolites from Ascension Island.....	34
3-8 CIPW norms of dacites and rhyolites from Ascension Island.....	37
3-9 Climatology for Ascension Island AAFB.....	47
3-10 Radiocarbon data for sample of bioclastic beach sand.....	51
3-11 K-Ar data for samples from Ascension Island.....	52
4-1 Statistics of Radon Track Etch Surveys.....	57

## PLATES

- Plate I - Geologic map of Ascension Island
- II - Geologic cross sections of Ascension Island
- III - Sample and survey location map

## 1.0 EXECUTIVE SUMMARY

This report details the technical geologic work which has been done under Phase I of an evaluation of the geothermal potential of Ascension Island. A more general report published previously (September, 1982) outlined our conclusions, and this document is intended for presentation of the technical data and more detailed discussion of the geology.

Ascension Island is a geologic anomaly. It was initiated by volcanism along the Mid-Atlantic Ridge about 7 million years ago, and that volcanism has continued as the oceanic plate has moved westward away from the median valley of the ridge. There are no other islands or seamounts in its vicinity to record similar volcanic activity. In this report we draw on data from Hawaii and Iceland to propose a history of development and also speculate on the effects of island subsidence and alteration on the physical properties of rocks in the subsurface.

Geologic mapping performed during Phase I has documented the distribution and age relationships of lithologies and structures. Chemical analyses of rock samples have complemented the geologic mapping and have allowed a quantitative classification of rock types. The chemistry demonstrates smooth curves on variation diagrams pointing to systematic differentiation processes at depth, probably fractionation in high-level magma chambers. The presence of magma chambers, particularly trachytic magma chambers, is very positive evidence for the existence of a viable high-temperature geothermal system on Ascension Island.

Radiometric dating of trachytic units on Ascension Island has demonstrated that most of the exposed rocks are younger than 1 million years. It has also shown that Devil's Cauldron is the youngest trachytic



feature on the island and is in fact too young to be dated by K-Ar methods. The most recent basaltic volcanism on the western side of the island is extremely young, probably on the order of hundreds of years. In addition, the volumes of erupted material are extremely large, suggesting the high potential for heat sources in the South Gannet Hill and Sisters Peak areas.

We have concluded from our preliminary examination that the potential for a geothermal discovery on Ascension Island is very high. In fact, we believe it to have one of the highest geothermal potentials of any unexplored area in the world today. In light of this conclusion, an exploration strategy is recommended for Phase II of the project.

Because of interest expressed by USAF personnel, we have made some comments about volcanic hazards on Ascension island. At this time, the probability of an eruption is quite small. We feel that any future volcanic eruptions would be preceded by earthquakes and surface thermal activity.

## 2.0 INTRODUCTION

Geothermal systems, utilizing the natural heat of the earth, are commonly classified according to temperature. High-temperature systems are those with base temperatures above 150°C, while systems of 90°-150°C are characterized as intermediate-temperature, and those of less than 90°C are termed low-temperature (White and Williams, 1975). Using existing technologies, only high-temperature resources are suitable for the generation of electrical power. However, low- and intermediate-temperature fluids can be applied to direct heat uses.

It has also become common practice to classify systems as vapor-dominated or liquid-dominated (White et al., 1971). Briefly, a liquid-dominated geothermal system uses water as the heat transporting medium. A vapor-dominated system uses water vapor to transport heat and is believed to be formed in areas where discharge exceeds recharge of a water-dominated system so that vapor-dominated zones form through boiling and lowering of the water table.

A geothermal resource requires three components: a heat source, fluids to transport the thermal energy, and permeability within the host rocks to form fluid pathways. In the case of a young volcanic island like Ascension, the heat source would be molten rock, or crystallized but still hot rock at a shallow depth. The fluid component could either be derived from sea water or meteoric water. Permeability of the host rocks could be a result of either the original textures in the rock or later faults and fractures. Geothermal systems are often manifested at the surface by hot springs or fumaroles. However, these features are not present on Ascension Island. Therefore, our examination concentrated on the evidence for heat, subsurface fluids, and

permeability.

The geologic field work for Phase I of the project was done between 8 July and 29 July, 1982. This technical report details the geologic work done on the island and results of subsequent laboratory studies. These results were summarized previously in a general Phase I report from the ESL/UURI and EG&G, Idaho team dated September, 1982.

### 3.0 GEOLOGY OF ASCENSION ISLAND

#### 3.1 Regional Setting

Ascension Island is composed almost entirely of volcanic rocks with minor alluvium and limited bioclastic beach sand deposits. The island is the top of a volcanic mountain which rises 4 km above the sea floor and is 50 km in diameter at its base.

Ascension Island is located about 100 km west of the Mid-Atlantic Ridge median valley and 50 km south of the Ascension fracture zone (van Andel et al., 1973). The Ascension fracture zone trends N78°E and has about 270 km of right-lateral offset relative to the ridge's median valley (Fig. 3-1). The Mid-Atlantic Ridge is a global structure which extends from Iceland to south of Africa and is the site of formation of new ocean crust. High heat flow and volcanic activity are typical along the ridge (van Andel, 1968; Quintino and Machado, 1977). In addition to the igneous activity localized at the crest of the ridge, a few volcanic centers continue to be active as the oceanic plate moves away from the ridge crest. Iceland, the Azores, Tristan da Cunha, and Ascension Island are examples of localized volcanic activity associated with the Mid-Atlantic Ridge.

van Andel et al. (1973) show that Ascension Island lies across magnetic anomaly 4 of Heirtzler et al. (1968). Thus the sea floor on which Ascension Island sits was being formed at the median valley approximately 7 m.y. ago. They also report that bathymetry demonstrates that Ascension is a solitary island without other islands or seamounts in its vicinity.

#### 3.2 Island Development

Until drilling is underway on this project we can only speculate on the subsurface geology of Ascension Island. It is, however, important to have an

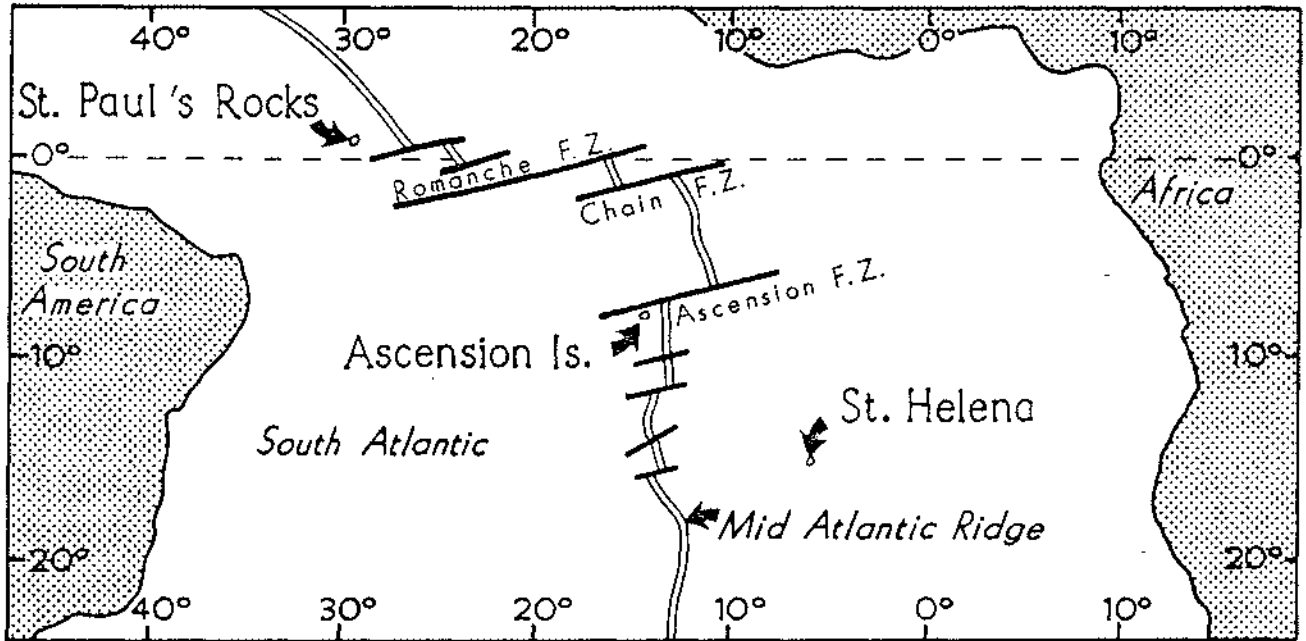
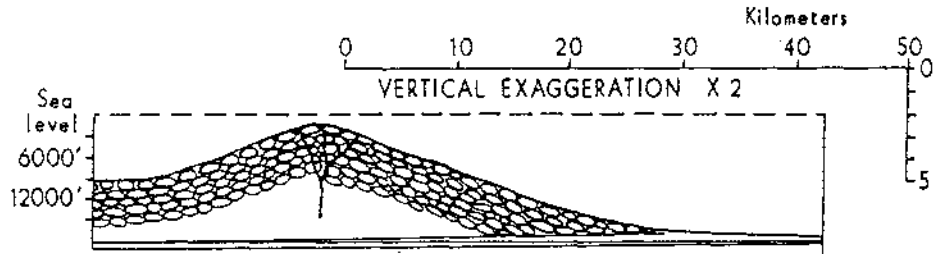


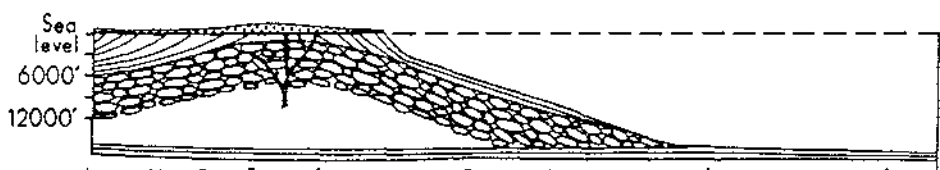
Fig. 3-1 Location of Ascension Island, the Mid-Atlantic Ridge and ocean fracture zones.

idea of the subsurface geology to conceptualize models of geothermal systems and for the practical value of predicting the types of rocks to be encountered in drill tests. Numerous authors have discussed island development and presented data from deep drilling operations on oceanic islands. A general model for island development is suggested by the work of Moore and Fiske (1969) which specifically concerned the island of Hawaii. Figure 3-2 is adapted from their work and applied to the genesis of Ascension. In addition to, and contemporaneous with, the establishment of a volcanic pedestal, island systems undergo subsidence due to plate motion and isostatic adjustments. Also, the volcanic rocks undergo metamorphism due to burial and magmatic heat input. These factors will affect the permeability and heat distribution of associated geothermal systems.

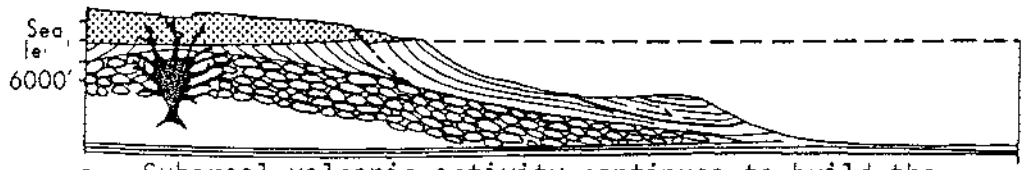
The initial eruptions forming Ascension Island took place in the median valley of the Mid-Atlantic Ridge. At water depths greater than 2 km, which was certainly the case with Ascension, water pressure inhibits vesiculation of the lavas and thus the principal rock type forming the base of the pedestal would be largely pillow basalts (Fig. 3-2a). As the volcanic pile builds near the surface of the sea, vesiculation increases and the rocks are shattered by contact with the cold sea water, producing fragmental rocks termed hyaloclastites. As with subaerial fragmental rocks, the hyaloclastites are able to maintain steeper slopes than flows. However, the rocks are less stable than the lava flows, and debris flows and turbidity currents are undoubtedly common at this stage of development. When the developing island reaches wave base (Fig. 3-2b), the rate of accretion must be greater than the rate of erosion plus rate of subsidence for the volcanic pile to grow above sea level and establish itself as an island. Once the island has been established, it is built up by the subaerial volcanism which is easily



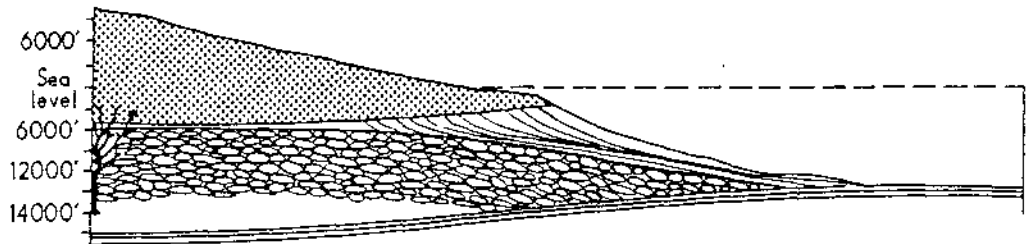
a. Volcanic pedestal established by eruption of pillow basalts along median valley of Mid-Atlantic Ridge. The volcanism continues as the oceanic plate moves to the west away from the median valley.



b. Hyaloclastites are formed as eruptions occur in shallower water. Subareal volcanism establishes the island above sea level.



c. Subareal volcanic activity continues to build the island. Isostatic adjustment results in depression of subareal volcanics below sea level.



d. The island grows through volcanic eruption, and isostatic sinking continues. Metamorphism has begun to affect the subareal volcanic rocks.

Fig. 3-2 Conceptual model for the development of Ascension Island (modified from Moore and Fiske, 1969).

observed at Ascension and which will be described in subsequent sections of this report.

The volcanic island represents an anomalous mass which is developed through time on the oceanic plate. As a result of loading of this mass upon the oceanic crust, subsidence takes place through isostatic adjustment. In addition, the oceanic crust moves into deeper water as it moves away from the Mid-Atlantic Ridge (Menard, 1969). As a result of this sinking, subaerial volcanic rocks subside below sea level (Fig. 3-2c and d). In addition, about 100 meters of sea level rise can be attributed to Pleistocene deglaciation (King, 1966). Deep drilling on Sao Miguel Island in the Azores has found subaerial extrusive rocks at depths of over 700 m below sea level (Muecke et al., 1974). Deep drilling at Reydarfjordur, Iceland has encountered subaerial volcanic rocks at nearly 2 km below sea level (Robinson et al., 1982).

Subaerial volcanic rocks are more permeable than submarine pillow basalts and hyaloclastites. Their occurrence in the subsurface will thus have important implications for the near-surface hydrology and recharge of a geothermal system as well as the reservoir controls of any geothermal system. Other factors which will affect subsurface permeability are metamorphism and hydrothermal alteration of the volcanic rocks with depth.

Studies of metamorphism and hydrothermal alteration in Iceland have shown the existence of broad regional metamorphic zones (Walker, 1960). With increasing depth the unaltered basalt flows enter a chabazite-thompsonite zone, an analcime zone and a mesolite-scolecite zone. Superimposed upon these regional features are local areas of alteration around active geothermal areas and older volcanic centers.



Mehegan et al. (1982) have studied alteration in the Iceland Research Drilling Project (IRDP) hole in Reydarfjordur. This hole encountered a fossil hydrothermal system. The authors' description is quoted below directly because it not only discusses the mineralogic changes but also the accompanying textural changes.

Three distinct stages of alteration and mineralization can be recognized in the drill core. The first involves prograde alteration of primary minerals and open-space mineralization in the lava flows, with increasing intensity with depth. As the temperature increased downward, some of the early secondary minerals were dissolved, producing relatively large cavities and vugs. In the second stage the system was gradually cooling down, and lower-temperature authigenic minerals were precipitated into the dissolution cavities. Superimposed on these earlier stages is an episode of vein mineralization and local contact metamorphism associated with late stage intrusion of the dikes into the lava pile. This stage is characterized by the formation of andradite garnet adjacent to dike margins.

In the upper part of the core to a depth of about 1200 m, alteration is characterized by open-space mineralization with little alteration of primary minerals. Olivine and interstitial glass are usually altered, but plagioclase and clinopyroxene are little affected. Common mineral assemblages are clay minerals  $\pm$  calcite  $\pm$  quartz  $\pm$  laumontite, but several other zeolites are also present in small quantities. Alteration in the lower part of the core is characterized by dissolution and replacement of primary minerals and earlier authigenic minerals as well as later open-space filling. Two principal assemblages are recognized: an early assemblage of epidote + quartz  $\pm$  chlorite  $\pm$  prehnite  $\pm$  albite and a later superimposed assemblage of laumontite  $\pm$  calcite  $\pm$  anhydrite. At the base of the drilled section, alteration is so intense that even the most impermeable rocks are severely affected.

The distribution of secondary minerals in that drill hole is shown in Fig. 3-3. Mehegan et al. (1982) also note that the effects of this alteration are most intense in flow breccias and fractures where permeability was the highest. Alteration was apparently never responsible for the complete elimination of permeability in the flow rocks. However, volcaniclastic rocks have often become sealed by the alteration. It is probable that similar metamorphic and alteration effects will be found in the subsurface of Ascension.

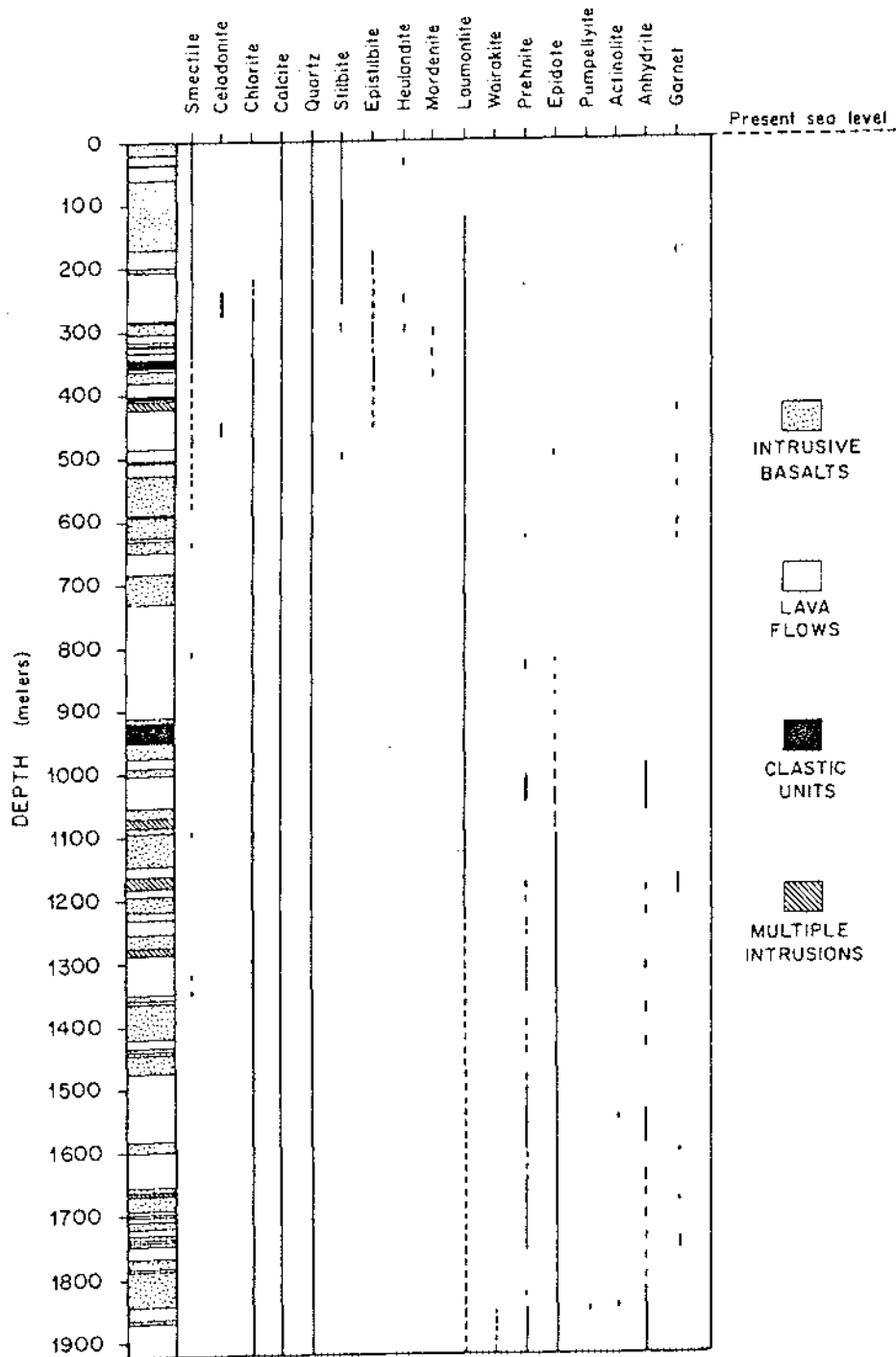


Fig. 3-3 Secondary mineral zonation in the IRDP hole (Mehegan et al., 1982).

The physical properties of the volcanic rocks will also change as a function of burial and alteration. Although we will not know the nature of these changes with certainty until drilling is underway, data from other explored areas can provide us with some insight into what we can expect to find. Again, much of our data comes from the detailed work on the IRDP hole. Oxburgh and Agrell (1982) have made thermal conductivity measurements on the core and their results are summarized in Figs. 3-4 and 3-5. As can be seen, there is an increase in thermal conductivity with depth largely reflecting the decrease in voids but also being somewhat controlled by mineralogic changes associated with alteration.

Changes of natural magnetization of samples can also be expected with depth. This will be important to the Ascension project in interpreting the aeromagnetic data of Phase II. Variations in magnetization in the IRDP hole have been studied by Bleil et al. (1982) and are summarized in Fig. 3-6. They have found that magnetic susceptibility increases with depth to about 2 km and then decreases to the bottom of the drill hole. The initial increase cannot be explained, but the decrease with depth is thought to be a result of metamorphic reactions. This decrease is linear enough that the authors have projected a zero magnetic susceptibility at a depth of about 4.3 km. This depth is just below that predicted for the onset of greenschist facies metamorphism. Also in the section studied, secondary magnetite was produced in epidote-bearing flows at depths greater than about 2.8 km. This development of secondary magnetite is correlated with an increase in dike density and is probably a contact metamorphic phenomenon. We expect that an analogous situation exists at Ascension Island and will enable us to identify subsurface dike swarms by their magnetic signature.

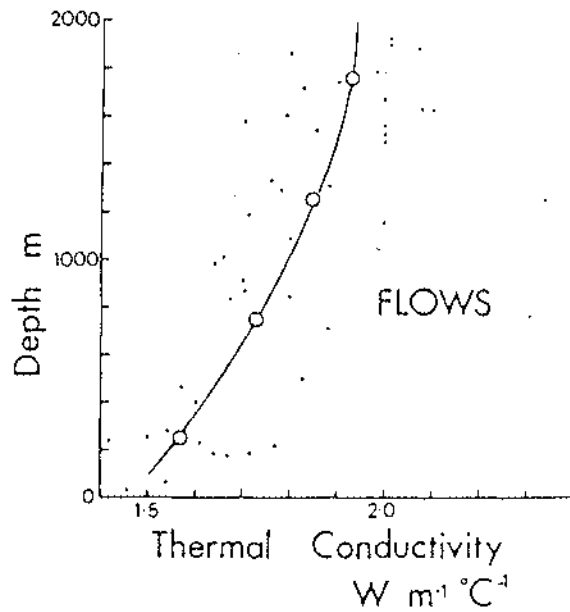


Fig. 3-4 Thermal conductivity as a function of depth for basalt flows in the IRDP hole (Oxburgh and Agrell, 1982).

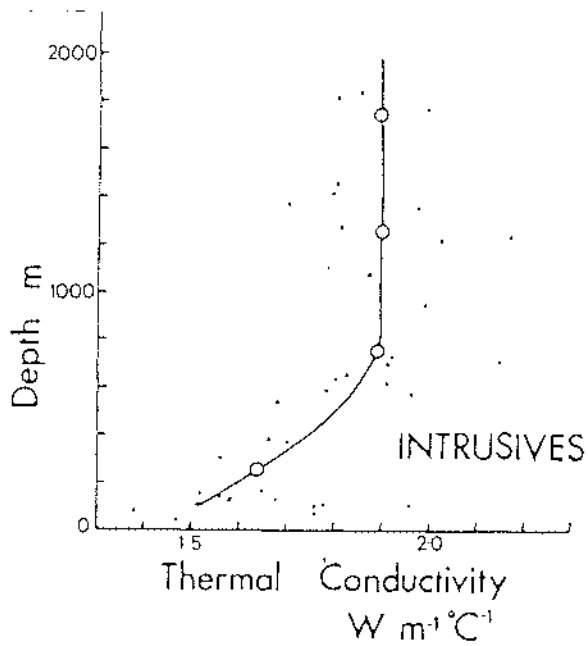


Fig. 3-5 Thermal conductivity as a function of depth for basaltic hypabyssal intrusives in the IRDP hole (Oxburgh and Agrell, 1982).

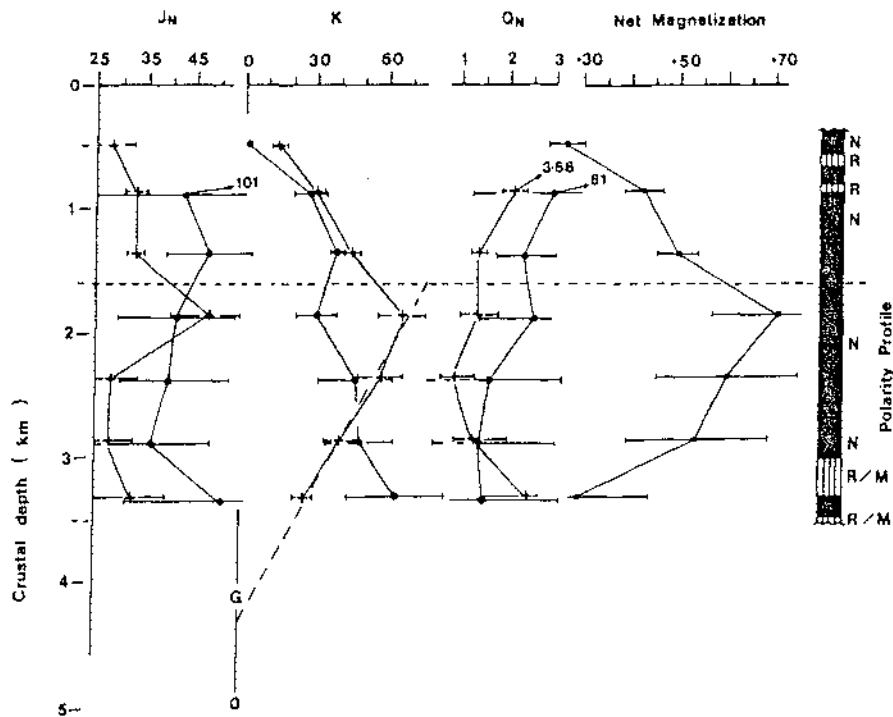


Fig. 3-6 Variation with depth of natural remnance ( $J_n$ ,  $\times 10^4$  cgs), initial susceptibility ( $k$ ,  $\times 10^4$  cgs), Königsberger ratio ( $Q_n$ ), and net magnetization ( $\times 10^4$  cgs) in the IRDP hole expressed as weighted averages for 500-m depth intervals; pluses, flow values; dots, dike values. G indicates estimated depth of onset of greenschist facies metamorphic conditions. Horizontal line is level of drill collar. Inclined dashed line is the regression line for the four deeper flow susceptibility values (Bleil et al., 1982).

### 3.3 Island Geology

#### 3.3.1 Introduction

Phase I field work on Ascension was devoted to the construction of a detailed geologic map of the island. This was done for the following reasons:

1. Geologic mapping is a means of systematically documenting geologic observations such as rock type, age relationships, faults, and evidence of geothermal activity.
2. The map serves as "ground truth" for the planning of subsequent exploration activities. The geologic map developed during Phase I is included in this report as Plate I and is described in this section.

Our mapping expands greatly upon the detail presented by R. A. Daly (1925) and Atkins et al. (1964). The volcanic rocks exposed on the surface of Ascension Island are samples of rocks which, at depth, may still be molten or very hot. These buried intrusive bodies would be sources of heat for any geothermal system on Ascension. Smith and Shaw (1975) have reasonably concluded that geothermal resources associated with felsic volcanic rocks younger than one million years have a potential for being high temperature. This relationship reflects the ability of molten granitic bodies to reside within the upper portions of the crust while they cool. Basaltic magmas, by contrast, undergo rapid transport from their area of generation and are more likely to be erupted at the surface as flows rather than forming high-level intrusive bodies. Thus one exploration criterion for high-temperature geothermal systems is their association with felsic volcanic rocks of less than one million years in age. Examples of such systems are Yellowstone National Park, Wyoming, Jemez Mountains, New Mexico, Long Valley and Coso,

California, Roosevelt Hot Springs, Utah, and Steamboat Hot Springs, Nevada. Young basalt provinces are of high potential if they are less than several thousand years old and if they show evidences of differentiation to more felsic end members. Examples of geothermal systems associated with this environment are found in the Azores, Iceland, and Hawaii.

The general Phase I report for this project utilized the rock nomenclature which had been presented by previous authors (Daly, 1925; Atkins et al., 1964), who had mapped the rocks as either basalts or trachytes. In previous work, the name trachyte was used in the general sense, that is "fine-grained, generally porphyritic extrusive rocks having alkali feldspar and minor mafic minerals as the main components" (AGI Glossary of Geologic Terms). The basalt-trachyte classification was maintained to simplify the geologic discussion in our general report. We will continue to use the term trachyte in its more general context, but where possible we will use more precise definitions of rock types.

Due to the fine-grained nature of volcanic rocks, classification is most accurately based on chemistry. For the purpose of this discussion, felsic rocks will be classified according to the scheme of Ewart (1979), which is shown in Fig. 3-7. Other workers have used in the past, and will continue to use, different nomenclature for the classification of igneous rocks like those that are found on Ascension Island. The rock names hawaiite, mugearite, benmoreite, and comendite are often used in the literature and are quite acceptable although they are generally not part of the layman's vocabulary. We have not at this time modified the geologic map to reflect any terminology changes.

Chemical analyses of the rocks of Ascension Island will be presented as

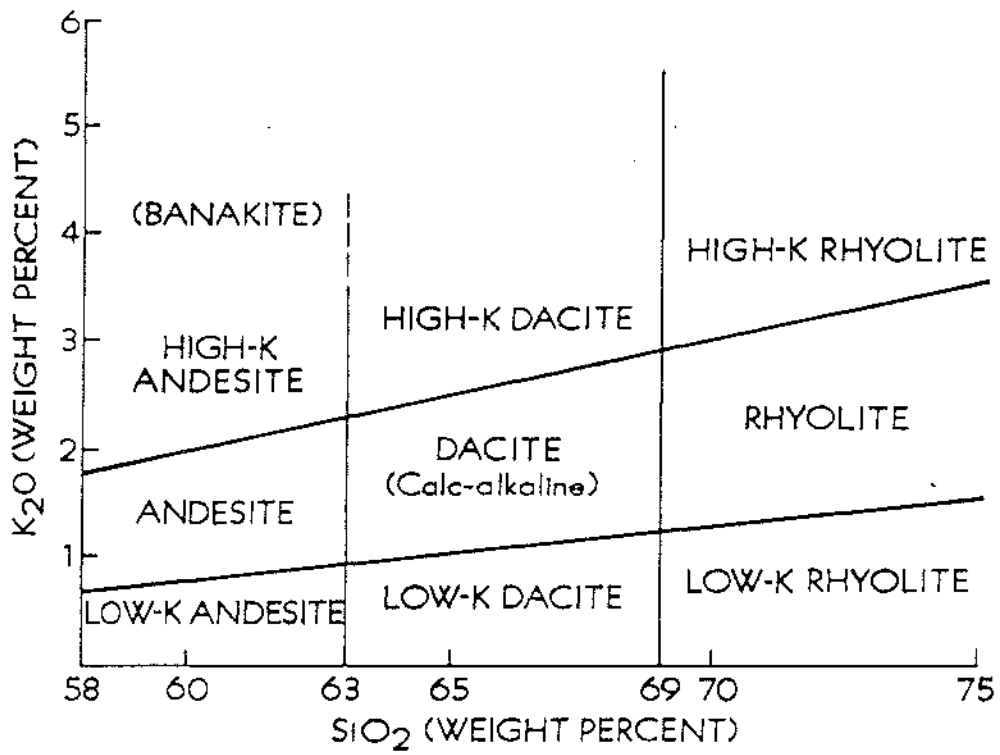


Fig. 3-7 Classification of andesite, dacite, and rhyolite by K<sub>2</sub>O and SiO<sub>2</sub> contents (Ewart, 1979).



the rocks are discussed. The new analyses presented in the report have been analyzed by methods described by Christensen et al. (1980). In general, the volcanic rocks of Ascension are slightly alkaline in character and form a rather continuous series as shown in the total alkali-silica diagram of Fig. 3-8. This diagram contains 37 analyses of rocks from Ascension which come from both the published literature and from the analyses done as a part of this study. Another way of looking at the composition of rocks from Ascension is by using the AFM plot which is shown in Figure 3-9. We will not present a detailed analysis of the trends shown in Figures 3-8 and 3-9 in this report. However, it can be stated that the diagrams are compatible with the derivation of the rocks through crystal fractionation. This implies the presence of magma chambers beneath Ascension Island which are the types of heat sources we desire for a viable high-temperature geothermal system.

Because of the uncertainties of relative ages of many of the rocks on Ascension and the importance of rock type and ages on the geothermal potential, the geology of the island will be discussed by rock type and relative age relationships.

### 3.3.2 Basalts

Most of the youngest igneous activity on Ascension Island has involved the formation of basalt flows (bf<sub>1</sub> on Plate I) with less voluminous formation of basaltic cinder cones. Additional fissure eruptions in the Letterbox area east of White Hill have involved the formation of andesite flows and pyroclastics and will be discussed in a subsequent section of this report. The distribution of these young flows is shown in Figure 3-10.

The most voluminous of the youngest flow sequences have flowed out of vent areas to the north, northwest, and south of Sisters Peak (Fig. 3-10).

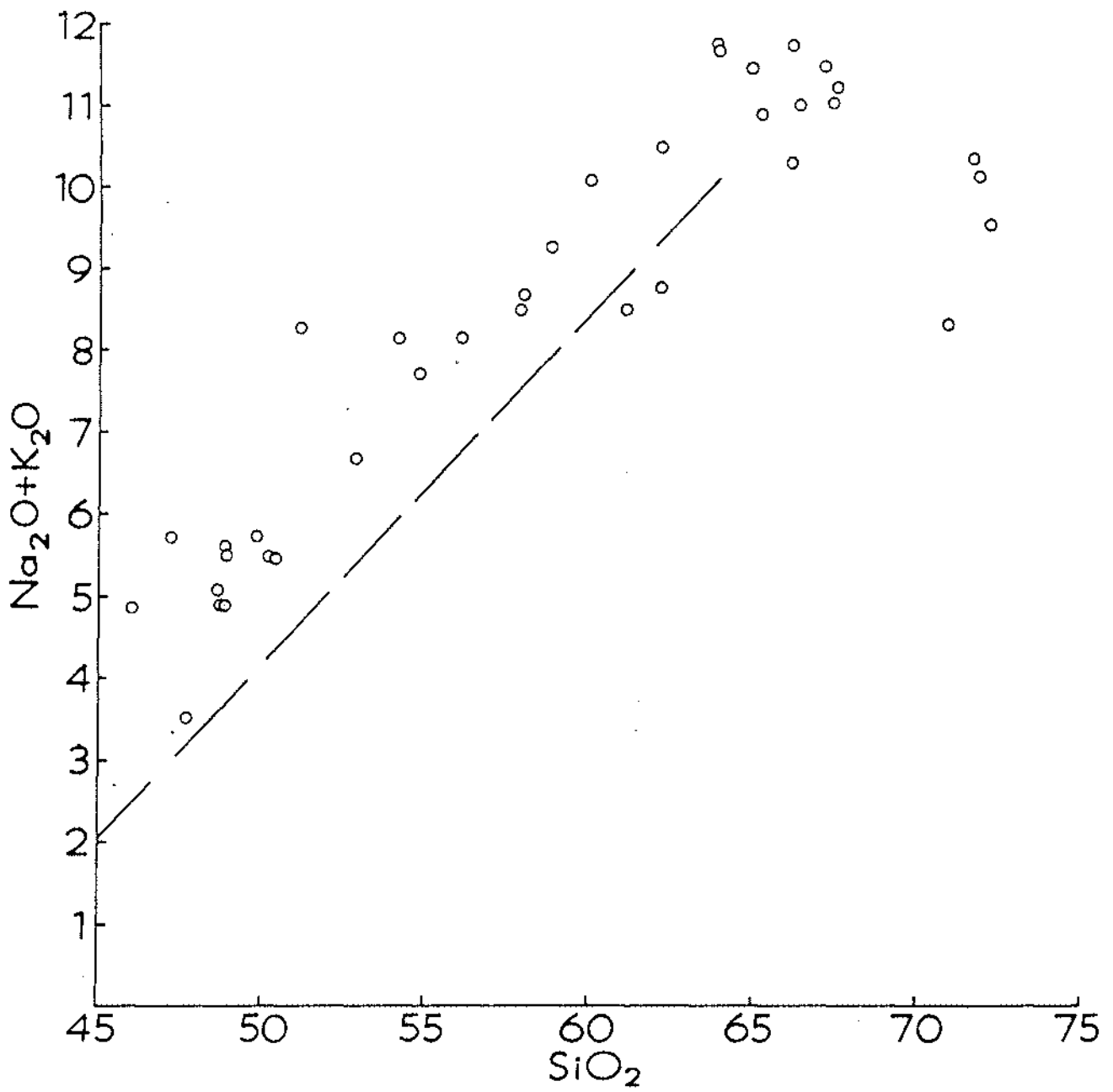


Fig. 3-8 Total alkali-silica diagram for rocks of Ascension Island. Dashed line is for reference and divides the alkaline and subalkaline fields (MacDonald, 1968).

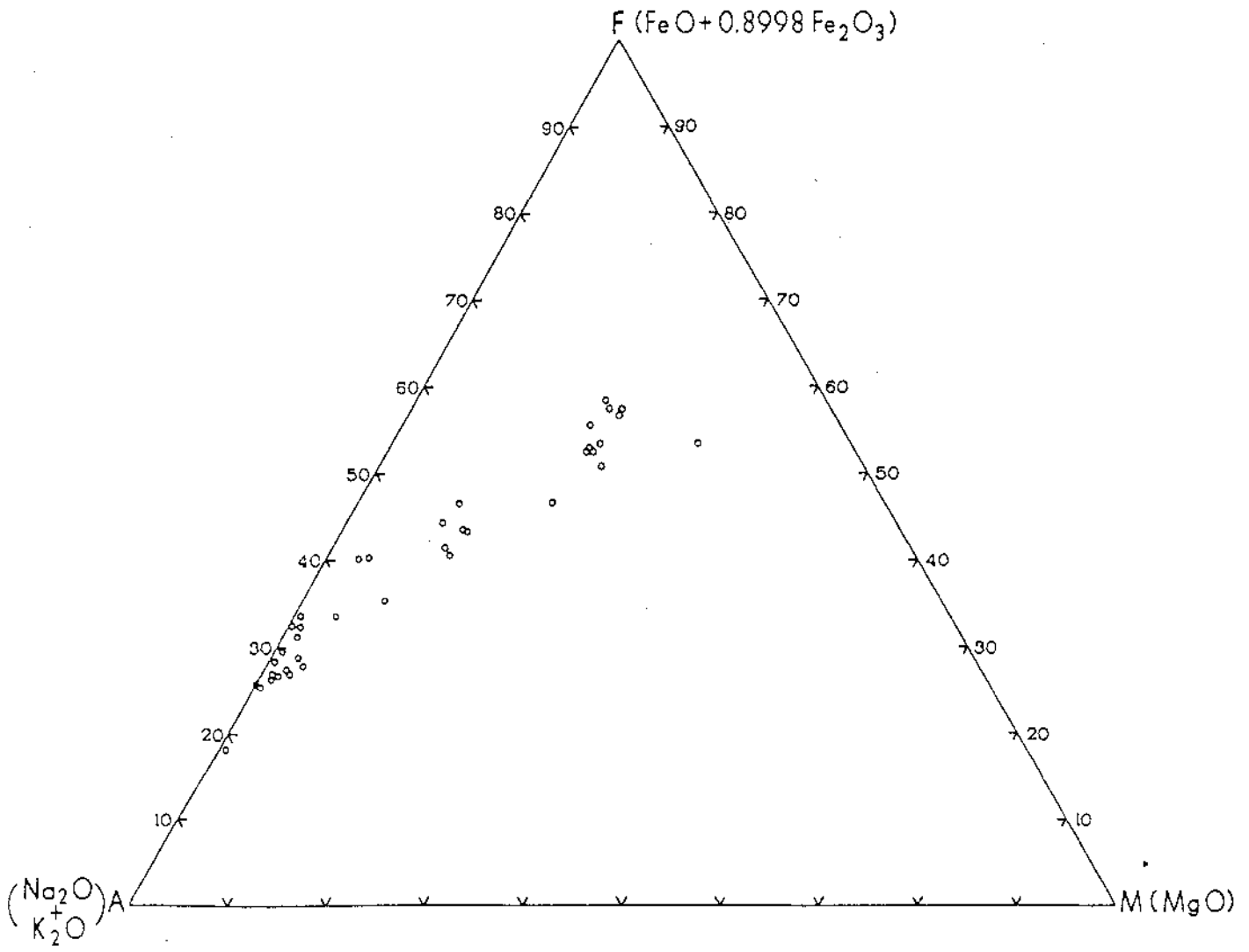


Fig. 3-9 AFM diagram of rocks from Ascension Island.

These flows were preceded by cinder eruptions to the northwest of Sisters Peak, and the flow activity has probably been responsible for the collapse of the cinder cone, leaving Sisters Peak as the highest remaining vestige. These flows were preceded by important eruptions from Broken Tooth and Hollow Tooth Craters (Plate 1).

Thin sections of these flows from Sisters Peak show that the rocks are olivine basalts. Chemical analyses are presented in Table 3-1 and CIPW norms are given in Table 3-2. In thin section, these rocks are somewhat monotonous with abundant small plagioclase phenocrysts and equant olivine phenocrysts. The rocks are vesicular and form flows that develop very blocky surfaces. In the immediate vicinity of vents, some ropey surfaces have developed where the eruptive materials were hottest. In addition, ponding of lava at the vent areas was quite common.

The flows from the Sisters Peak area have vented from a number of different points about the same time. Since there is little infilling of the flow surface with ash to the northwest of Sisters Peak, the flow event undoubtedly postdated the ash and cinder eruption from the northwest end of Sisters Peak. This seems to be a common succession of events throughout the western part of the island, that is, an eruptive event was initiated by pyroclastic activity and the development of cinder cones and was then followed closely by basalt flows from the top, or more often, the base of the constructed cinder cone.

The Sisters event has a great deal of significance for geothermal exploration because a) it is very young, b) the volume of magma erupted was quite high, and c) the eruptions took place along what we interpret to be a broad zone of northwest-trending fractures. The youth and the volume of the

flows suggest to us that the feeder systems for these flows are still hot and able to provide heat to circulating geothermal fluids. The strong structural controls suggest that, at depth, the feeder system probably forms a series of northwest-trending dikes which, with greater depth, may make up the predominant volume of the rock. Such dike swarms have been proposed for vent areas in Iceland and Hawaii.

The other major young basalt vent area is located on the southeast side of South Gannet Hill near the Wideawake Airfield. The degree of weathering of the flow surface suggests that this event is approximately the same age as the flows of the Sisters Peak area. As was the case to the north, this flow also closely followed the emplacement of other basalt flows in the area and was controlled by structural zones. These structural zones have a southwest trend and also control the locations of the vent areas of the older flows such as those from Booby Hill and the voluminous flow from the base of Spoon Crater (Plate I). Petrologically the South Gannet Hill flow is quite similar to the flows to the north around Sisters Peak. Petrochemically (Table 3-1) the flow is more alkaline than the flows to the north.

Another area of young basaltic activity is located on the northeast side of the island, north of Devil's Cauldron. No analysis of this rock is presently available, however, thin section examination shows that the rock may be an andesite rather than a basalt. Mapping (Plate I) has demonstrated that the eruption of this flow was controlled by a north-south-trending fracture zone. This fracture projects into the Devil's Cauldron area which, as will be discussed in a subsequent section, is the youngest felsic eruptive center on Ascension Island.

Basalt flows, which are slightly older than the most recent events

Table 3-1 Whole rock chemical analyses of basalts from flows around Sisters Peak and South Gannett Hill. Major element analyses are expressed as weight percent and trace elements are in parts per million.

	AI-82-2	AI-82-14	AI-82-18	AI-82-19	AI-82-28	AI-82-32
SiO <sub>2</sub>	50.4	50.2	48.62	49.9	48.8	46.0
Al <sub>2</sub> O <sub>3</sub>	15.23	15.11	15.15	15.56	15.75	15.78
FeO*	10.68	10.38	13.06	11.13	11.04	12.83
MgO	4.11	4.65	4.58	4.31	4.24	4.90
CaO	7.36	7.63	8.75	7.86	7.87	9.26
Na <sub>2</sub> O	3.91	3.92	3.74	4.17	4.06	3.59
K <sub>2</sub> O	1.50	1.52	1.34	1.59	1.54	1.23
MnO	0.21	0.21	0.24	0.20	0.22	0.20
TiO <sub>2</sub>	2.99	3.04	3.39	2.97	3.04	3.64
P <sub>2</sub> O <sub>5</sub>	0.94	0.94	1.12	0.98	1.13	1.02
LOI	0	0	0	0	0	0
	<u>97.33</u>	<u>97.60</u>	<u>99.99</u>	<u>98.67</u>	<u>97.69</u>	<u>98.45</u>
Sr	460	389	450	470	411	360
Ba	37	37	32	36	39	29
Co	19	21	20	20	20	32
Ni	<5	<5	<5	<5	5	19
Cu	13	16	19	11	15	35
Pb	<10	<10	<10	<10	<10	<10
Zn	108	18	136	110	115	104
Li	5	5	3	4	5	5
Be	1.8	1.6	1.7	1.7	1.6	1.3
Zr	307	244	264	293	254	181
La	31	30	28	29	32	2.5
Ce	40	50	37	36	57	39

1. AI-82-2 Olivine basalt plug south of Sisters Peak
2. AI-82-14 Olivine basalt from vent area on north side of Sisters Peak
3. AI-82-18 Olivine basalt from uplifted blocks in vent area on south side of Sisters Peak
4. AI-82-19 Olivine basalt from vent area on south side of Sisters Peak
5. AI-82-28 Olivine basalt from vent area along English Bay Road
6. AI-82-32 Olivine basalt from vent area on southeast side of South Gannett Hill

\*Total Iron calculated as FeO

LOI is loss on ignition

TABLE 3-2 CIPW norms of basalts from flows around Sisters Peak and South Gannet Hill. (See Table 3-1 for locations). Norm calculations use the following abbreviations: Q = quartz, Or = orthoclase, Ab = albite, An = anorthite, Ne = nepheline, Di = diopside, Hy = hypersthene, Ol = olivine, Il = ilmenite, Ap = apatite.

	AI-82-2	AI-82-14	AI-82-18	AI-82-19	AI-82-28	AI-82-32
Q	0	0	0	0	0	0
Or	8.86	8.98	7.92	9.40	9.10	7.27
Ab	33.09	33.17	31.78	35.29	34.35	24.78
An	19.58	19.14	20.41	19.04	20.20	23.31
Ne	0	0	0.11	0	0	3.03
Di	9.05	10.47	13.19	11.36	9.61	13.38
Hy	13.51	9.58	0	0.42	0.48	0
Ol	5.39	8.29	17.58	15.25	15.55	17.40
Il	5.68	5.77	6.44	5.64	5.77	6.91
Ap	<u>2.23</u>	<u>2.23</u>	<u>2.65</u>	<u>2.32</u>	<u>2.68</u>	<u>2.42</u>
TOTAL	97.38	97.65	100.09	98.72	97.75	98.50

discussed above, have been mapped as  $bf_2$  on Plate I. These include the flows of Broken Tooth and Hollow Tooth craters on the northern edge of the island, the flow which had its vent area on Donkey Plain southwest of Lady Hill, the flow which vented from near the base of Spoon Crater and flowed to the south, and flows which are exposed beneath  $bf_1$  in the Sisters Peak area and emanated from vent areas which have been covered by the more recent flows. Chemical analyses of these rocks are presented in Table 3-3 and CIPW norms are given in Table 3-4.

All remaining basalts on Ascension have been grouped as belonging to older flows. This does not imply that they are of similar age, but rather that they are older than  $bf_1$  and  $bf_2$  and that, with local exceptions, it was not possible to determine mutual age relationships. As has been previously suggested, most of these flows were associated with and preceded by pyroclastic eruptions which led to the formation of basaltic cinder cones.

One of the more impressive and long-lived basaltic centers is located at 2000 feet elevation southeast of The Peak on Green Mountain. This is probably the eruptive center of a shield volcano which formed the flows and pyroclastic deposits in much of the southeast portion of the island. Dacite domes and flows probably developed on the flanks of this shield volcano much in the same manner as domes have formed on the flanks of Hawaiian volcanoes. Examples of this would be the Ragged Hill dome and the dacites that have formed at Coconut Bay.

Basaltic dikes are fairly common where erosion has cut deep enough to expose them. The dikes are 1 to 10 feet thick and a few are exposed for more than a thousand feet in length. Most of the dikes follow the major structural trends.



TABLE 3-3 Whole rock chemical analyses of other basalt flows from Ascension Island. Major element analyses are expressed as weight percent and trace elements are in parts per million.

	AI-82-27	AI-82-42	AI-82-26	<u>2731</u>	<u>2850</u>	<u>2839</u>
SiO <sub>2</sub>	54.8	48.8	48.80	47.69	48.64	52.87
Al <sub>2</sub> O <sub>3</sub>	17.73	15.48	14.88	16.23	15.54	16.68
Fe <sub>2</sub> O <sub>3</sub>				2.20	5.31	4.54
FeO	7.51*	11.76*	12.66*	9.93	7.73	4.79
MgO	2.12	4.05	4.27	7.15	4.96	3.92
CaO	4.53	7.89	8.23	10.02	9.03	7.32
Na <sub>2</sub> O	5.36	3.95	3.64	2.87	3.60	4.63
K <sub>2</sub> O	2.36	1.48	1.18	0.64	1.24	2.06
MnO	0.24	0.23	0.23	0.17	0.17	0.37
TiO <sub>2</sub>	1.64	3.38	3.62	2.79	3.52	2.01
P <sub>2</sub> O <sub>5</sub>	0.90	1.39	1.31	0.59	0.64	0.52
LOI	0.30	0	0	0.32	0.37	0.70
TOTAL	<u>97.49</u>	<u>98.41</u>	<u>98.82</u>	<u>100.60</u>	<u>100.75</u>	<u>100.41</u>
Sr	388	460	377			
Ba	63	37	35			
Co	17	23	20			
Ni	<5	<5	<5			
Cu	6	10	13			
Pb	28	<10	<10			
Zn	140	125	134			
Li	9	6	5			
Be	2.0	1.7	1.4			
Zr	410	251	232			
La	48	34	30			
Ce	94	66	54			

TABLE 3-3 (cont.)

	2784	2761
SiO <sub>2</sub>	54.04	51.18
Al <sub>2</sub> O <sub>3</sub>	19.58	21.41
Fe <sub>2</sub> O <sub>3</sub>	5.09	4.61
FeO	3.75	3.32
MgO	1.99	1.75
CaO	5.54	6.56
Na <sub>2</sub> O	4.70	4.72
K <sub>2</sub> O	3.48	3.53
MnO		
TiO <sub>2</sub>	0.94	1.34
P <sub>2</sub> O <sub>5</sub>	0.31	0.48
LOI	<u>1.16</u>	<u>1.08</u>
TOTAL	100.58	99.98

1. AI-82-27 Olivine pyroxene basalt from vent area southwest of Lady Hill
2. AI-82-42 Olivine pyroxene basalt from vent area south of Spoon Crater
3. AI-82-26 Basalt from Two Boats flow collected along Old Mountain Road
4. 2731 Olivine basalt, surface flow of southwest group (Daly, 1925)
5. 2850 Olivine-poor basalt flow, north wall of Cricket Valley (Daly, 1925)
6. 2839 Trachydoleritic basalt flow from Mountain Red Hill (Daly, 1925)
7. 2784 Trachydolerite from Hayes Hill (Daly, 1925)
8. 2761 Trachydolerite from Landing Pier cone (Daly, 1925)

TABLE 3-4 CIPW Norms of basalts from Ascension Island. (See Table 3-3 for locations.)

	AI-82-27	AI-82-42	AI-82-26	2731	2850	2839	2784	2761
Q	0	0	0	0	0	0	0	0
Cor	0.28	0	0	0	0	0	0	0
Or	13.95	8.75	6.97	3.78	7.33	12.17	20.56	20.86
Ab	45.35	33.42	30.80	24.28	30.46	39.18	39.77	32.24
An	16.59	20.14	20.78	29.51	22.58	18.65	22.05	26.81
Ne	0	0	0	0	0	0	0	4.17
Di	0	8.35	9.67	13.35	14.47	11.36	2.71	2.03
Hy	12.85	5.82	12.57	8.93	9.54	6.68	3.54	0
Ol	2.97	12.30	8.12	10.56	0.14	0.07	0.90	2.45
Mt	0	0	0	3.19	7.70	6.58	7.38	6.68
Il	3.11	6.42	6.88	5.30	6.69	3.82	1.79	2.54
Ap	<u>2.13</u>	<u>3.29</u>	<u>3.10</u>	<u>1.40</u>	<u>1.52</u>	<u>1.23</u>	<u>0.73</u>	<u>1.14</u>
TOTAL	97.23	98.49	98.89	100.30	100.43	99.74	99.43	98.92

### 3.3.3 Andesites

Several andesite flows have been mapped on Ascension Island. The most significant of those from the geothermal standpoint is the young fissure eruption which extends from White Hill to Letterbox in the far eastern end of the island. Here flows and pyroclastic rocks have been erupted from a clearly defined open fissure which has no appreciable offset along it. Chemical analyses and CIPW norms of these rocks are shown in Tables 3-5 and 3-6 respectively.

Andesites have also been mapped on the northern slopes of Green Mountain south of Bears Back. In addition, an analysis from Baker (1973) of a sample collected at the summit of Bears Back suggests that andesites may crop out there. The andesites exposed on the island are subordinate in volume to basalts and the dacites and rhyolites which will be discussed next. However, they do suggest the possibility of differentiation from basalt and thus the potential for heat sources at higher levels in the crust than would be the case with normal basaltic volcanism. Examination of thin sections of these rocks show them to be pyroxene andesites with abundant small plagioclase laths.

### 3.3.4 Dacites and Rhyolites

As has been mentioned previously, Daly (1925) and Atkins et al. (1964) have mapped the silicic rocks on Ascension Island as trachytes. This terminology was followed in our earlier summary report on this project and, as was mentioned previously, we will continue to use the term trachyte in its more general context. However, for this report and future technical work we will use the rock classification summarized in Fig. 3-7. Chemical analyses of these trachytic rocks are given in Table 3-7 and norms are presented in Table 3-8.

TABLE 3-5 Whole rock chemical analyses of andesites from Ascension Island. Major element analyses are expressed as weight percent and trace elements are in parts per million.

	AI-82-12	2864	As-9	15220
SiO <sub>2</sub>	57.9	58.00	61.2	62.26
Al <sub>2</sub> O <sub>3</sub>	17.13	14.92	15.43	15.95
Fe <sub>2</sub> O <sub>3</sub>		1.73		3.69
FeO	7.38*	5.78	6.08*	2.52
MgO	2.13	2.23	0.61	0.52
CaO	4.63	4.50	2.59	2.88
Na <sub>2</sub> O	5.77	5.88	5.44	5.84
K <sub>2</sub> O	2.70	2.76	3.05	2.94
MnO	0.24	0.11	0.21	0.20
TiO <sub>2</sub>	1.45	3.38	0.71	0.60
P <sub>2</sub> O <sub>5</sub>	0.67	0.71	0.53	0.60
LOI	0.15	0.40	0.95	1.55
TOTAL	<u>100.15</u>	<u>100.40</u>	<u>96.80</u>	<u>99.55</u>
Sr	424		230	
Ba	67		89	
Co	11		5	
Ni	<5		<5	
Cu	<5		7	
Pb	<10		<10	
Zn	134		143	
Li	7		12	
Be	2.5		2.5	
Zr	553		516	
La	41		43	
Ce	58		90	

1. AI-82-12 High-potassium andesite from young fissure eruption at Southeast Head
2. 2864 Trachyandesite flow from fissure, Southeast Head (Daly, 1925)
3. AS-9 High-potassium andesite from north side of Green Mountain
4. 15220 Benmoreite, summit of Bears Back (Baker, 1973)

\* Total iron calculated as FeO

TABLE 3-6 CIPW norms of andesite from Ascension Island (See Table 3-5 for locations).

	2864	AI-82-12	As-9	15220
Q	3.02	0	8.34	11.86
Qr	16.31	15.96	18.02	17.37
Ab	49.75	48.82	46.03	49.42
An	6.17	12.87	8.68	8.63
Di	9.41	4.86	0.62	1.41
Hy	4.76	9.43	11.58	1.26
Ol	0	3.75	0	0
Mt	2.51	0	0	5.35
Il	6.42	2.75	1.35	1.50
Ap	1.68	1.59	1.26	1.42
TOTAL	<u>100.03</u>	<u>100.03</u>	<u>95.88</u>	<u>98.22</u>

The trachytic rocks of Ascension Island are largely confined to the central and eastern portion of the island. In addition, there are exposures of felsic rocks on the north and south sides of Cross Hill and at the northwest end of Sisters Peak (Daly's Craigs), suggesting a wide distribution in the subsurface. In addition, felsic pumice and ash are widely distributed about the island forming an excellent time-stratigraphic unit. Daly (1925) discussed the trachytic rocks at great length and for more detail the reader is directed to that excellent paper.

The most conspicuous of the felsic features on the island are the rhyolite domes that form Wig Hill, White Hill, Weather Post, and Ragged Hill. The White Hill dome, for example, which is little altered by erosion, rises about 300 m (1000 feet) above its base. The large flow extending 2600 m (8,650 feet) from Devil's Cauldron to North East Point is 120 m (400 feet) thick. The felsic domes and flows are light to medium gray, weathering to white and tan, and are flow banded. Where preserved, they have gray or rust-colored pumice talus aprons.

Most of these flows and domes are sparsely porphyritic, typically containing about 3 percent 1-5 mm euhedral phenocrysts of microcline and some plagioclase (about An 30) and a trace of augite. The Ragged Hill and Coconut Bay bodies contain 20 percent K-feldspar phenocrysts. Domes are holocrystalline and lava flows hypocrySTALLINE with 30 percent or more glass. Most outcrops contain small, irregular vesicles. Generally the trachytes are unaltered in thin section, but a few have minor alteration of the matrix to clays and of the opaques to red hematite.

Intrusive domes have arched up basalt flows forming Bears Back and Devil's Riding School and a dacite dike is exposed just north of the

Table 3-7 Whole rock chemical analyses of dacites and rhyolites from Ascension Island. Major element analyses are expressed as weight percent and trace elements in parts per million.

	AI-82-10	AI-82-15	AI-82-16	AI-82-17	AI-82-24
SiO <sub>2</sub>	58.8	64.9	60.00	62.3	66.2
Al <sub>2</sub> O <sub>3</sub>	15.97	15.05	18.72	17.13	16.76
FeO*	5.75*	4.80*	5.53*	4.39*	4.77*
MgO	1.28	0.16	0.67	0.45	0.22
CaO	3.11	0.91	2.25	1.80	1.25
Na <sub>2</sub> O	5.71	6.87	6.73	5.92	6.23
K <sub>2</sub> O	3.51	4.54	3.40	4.51	4.04
MnO	0.20	0.22	0.21	0.17	0.15
TiO <sub>2</sub>	1.11	0.41	0.68	0.42	0.44
P <sub>2</sub> O <sub>5</sub>	0.40	0.05	0.19	0.08	0.38
LOI	0.40	0.19	0.84	3.18	0.78
TOTAL	<u>96.24</u>	<u>98.10</u>	<u>99.22</u>	<u>100.35</u>	<u>101.22</u>
Sr	232	33	305	171	124
Ba	143	99	96	104	99
Co	29	9	16	53	36
Ni	<5	<5	<5	<5	<5
Cu	9	<5	<5	5	5
Pb	<10	<10	<10	<10	<10
Zn	110	145	165	151	145
Li	5	12	12	6	9
Be	2.2	2.4	2.4	3.5	2.3
Zr	368	719	921	839	983
La	34	42	54	53	46
Ce	45	65	117	88	78

1. AI-82-10 Pyroxene andesite from Cocoanut Bay
2. AI-82-15 High-potassium dacite from Bears Back
3. AI-82-16 High-potassium andesite from Drip Dome
4. AI-82-17 Andesitic pumice
5. AI-82-24 High-potassium dacite from flow east of Mountain Red Hill

\* Total iron calculated as FeO.



Table 3-7 (continued)

	AI-82-29	AI-82-25	V-4	As-2	As-11
SiO <sub>2</sub>	67.5	63.81	63.98	71.6	66.4
Al <sub>2</sub> O <sub>3</sub>	15.3	15.93	16.00	12.58	15.04
Fe <sub>2</sub> O <sub>3</sub>			2.57		
FeO	3.82*	4.54*	2.12	3.53*	5.27*
MgO	0.11	0.36	.64	0.02	0.04
CaO	0.39	1.16	1.58	0.35	0.45
Na <sub>2</sub> O	6.23	7.16	6.45	5.57	6.00
K <sub>2</sub> O	4.97	4.60	5.18	4.82	5.00
MnO	0.32	0.22		0.13	0.19
TiO <sub>2</sub>	0.32	0.49	0.28	0.22	0.37
P <sub>2</sub> O <sub>5</sub>	0.13	0.09		0.01	0.18
LOI	0.41	0.18	0.61	0.51	0.41
TOTAL	<u>99.50</u>	<u>98.54</u>	<u>99.41</u>	<u>99.34</u>	<u>99.35</u>
Sr	8	24		2	3
Ba	24	20		7	33
Co	14	23		16	15
Ni	<5	<5		<5	<5
Cu	<5	<5		<5	5
Pb	<10	<10		<10	<10
Zn	155	158		220	165
Li	14	11		25	14
Be	2.7	2.8		6.2	2.5
Zr	1059	717		988	654
La	48	47		64	29
Ce	103	82		152	57

6. AI-82-29 High-potassium dacite from the Craigs
7. AI-82-25 High-potassium dacite from Cross Hill quarry
8. V-4 Trachyte of Cross Hill quarry (Daly, 1925)
9. As-2 High-potassium rhyolite from flow east of Middleton Ridge
10. As-11 High-potassium dacite from flow on west end of Green Mountain

\* Total iron calculated as FeO.

Table 3-7 (Continued)

	2855	2863	V-3	V-5	2861	VII-2	15146	15373
SiO <sub>2</sub>	65.18	66.98	66.12	67.05	71.88	70.99	70.61	72.22
Al <sub>2</sub> O <sub>3</sub>	15.91	14.30	15.51	15.43	12.85	14.84	13.22	12.91
Fe <sub>2</sub> O <sub>3</sub>	4.41	3.85	3.27	3.25	3.60	3.76	0.95	1.32
FeO	0.98	0.33	0.93	1.25	0.05	0.35	1.38	2.38
MgO	0.10	0.30	0.17	0.16	0.18	0.14	0.11	0.31
CaO	0.81	0.83	1.05	1.06	0.60	0.60	0.43	0.43
Na <sub>2</sub> O	6.24	6.76	6.31	6.12	5.32	5.94	5.71	4.77
K <sub>2</sub> O	4.60	4.34	5.40	5.32	4.78	2.40	4.77	4.75
MnO	0.17	0.21			0.29	tr	0.08	0.14
TiO <sub>2</sub>	0.44	0.89	0.22		0.25		0.14	0.24
P <sub>2</sub> O <sub>5</sub>	0.08	0.22		0.04	0.05		0	0.1
LOI	1.07	0.52	1.98	0.56	0.35	0.40	2.57	0.35
BaO		0.04						
ZrO <sub>2</sub>		0.13						
TOTAL	<u>99.99</u>	<u>99.70</u>	<u>100.96</u>	<u>100.24</u>	<u>100.20</u>	<u>99.42</u>	<u>99.97</u>	<u>99.92</u>

- 2855 11. Trachyte of Ragged Hill dome (Daly, 1925)  
2863 12. Trachyte of Southeast Head Dome (Daly, 1925)  
V-3 13. Trachyte from a point "north of Dark Slope Crater" (Daly, 1925)  
V-5 14. Trachyte from a point "halfway up Green Mountain" (Daly, 1925)  
2861 15. Quartz trachyte outflow from White Hill Dome (Daly, 1925)  
VII-12 16. Augite trachyte from Weather Post (Daly, 1925)  
15146 17. Comendite, Little White Hill (Baker, 1975)  
15373 18. Comenditic obsidian, Middletons Ridge (Baker, 1975)

TABLE 3-8 CIPW norms of dacites and rhyolites from Ascension Island.  
See TABLE 3-7 for locations.

	AI-82-10	AI-82-15	AI-82-16	AI-82-17	AI-82-24	AI-82-29	AI-82-25	V-4	As-2
Q	1.70	5.96	0	3.14	8.78	9.72	1.73	3.52	22.77
Cor	0	0	0.36	0	0.78	0	0	0	0
Or	20.74	26.83	20.09	26.65	23.87	29.37	27.18	30.61	28.48
Ab	48.32	52.14	56.95	50.09	52.72	51.03	56.33	53.46	37.87
An	7.58	0	9.92	6.85	3.72	0	0	0	0
Ns	0	1.39	0	0	0	0.39	0.99	0.98	2.15
Di	4.48	3.71	0	1.36	0	0.96	4.53	6.42	1.49
Hy	9.99	6.99	3.81	8.09	8.86	6.53	6.46	0	5.62
Ol	0	0	5.54	0	0	0	0	0	0
Mt	0	0	0	0	0	0	0	3.23	0
Il	2.11	0.78	1.29	0.80	0.84	0.61	0.93	0.53	0.42
Ap	0.95	0.12	0.45	0.19	0.90	0.31	0.21	0	0.02
TOTAL	95.87	97.92	98.38	97.17	100.47	98.92	98.36	98.75	98.82
	AS-11	2855	2863	V-3	V-5	2861	VII-2	15146	15373
Q	8.50	9.98	11.79	8.21	10.18	23.06	25.76	20.34	24.00
Cor	0	0	0	0	0	0	1.38	0	0
Or	29.55	27.18	25.65	31.91	31.44	28.25	14.18	28.19	28.07
Ab	49.53	52.80	49.39	49.72	49.75	39.49	50.26	41.45	39.96
An	0	1.80	0	0	0	0	2.98	0	0
Ac	0	0	6.88	3.24	1.79	4.87	0	2.75	0.35
Ns	0.29	0	0	0	0	0	0	0.87	0
Wo	0	0.41	0	1.69	1.73	0.59	0	0	0
Di	0.94	0.54	1.37	0.91	0.86	0.97	0	1.87	1.79
Hy	9.02	0	0.11	0	0	0	0.35	1.58	3.09
Ol	0	0	0	0	0	0	0	0	0
Mt	0	2.44	0	3.00	3.74	0.38	1.13	0	1.74
Il	0.70	0.84	1.15	0	0.19	0.47	0	0.46	0.46
Hm	0	2.73	1.47	0.08	0.05	1.65	2.98	0	0
Ap	0.43	0.19	0.52		0	0.12	0	0	0.02
Tn			0.70						
TOTAL	98.96	98.91	99.03	98.76	99.73	99.85	99.02	97.51	99.48

Residency. The exposures west of Sisters Peak and near Cross Hill may also be of intrusive origin. Petrographically these near-surface intrusions are similar to the extrusive trachyte except they lack flow-banding.

### 3.3.5 Xenoliths

Before leaving the discussion of the volcanic rocks of Ascension, some comment should be made about the presence of the xenoliths these rocks contain and their significance for the geothermal exploration program. Xenoliths were collected and described by Darwin (1876), Daly (1925), and most recently by Roedder and Coombs (1967). In addition, the mineral dalyite was discovered and first described in xenoliths from Ascension (Van Tassel, 1951).

Xenoliths are abundant in the basalts of Dark Slope Crater and the felsic pyroclastics which are exposed on Green Mountain, and between Middleton Ridge and the NASA road. There is a zonation to the occurrence of these xenoliths that suggests differences in the rocks at depth beneath Ascension or, alternatively, reflecting different depths of origin of the xenoliths.

The xenoliths from Dark Slope Crater are up to a foot across. The rocks are coarse-grained and contain olivine + clinopyroxene + plagioclase + opaques. Peridotites, dunites, and plagioclase cumulates were observed in thin section and suggests that these rocks were derived from a layered mafic complex.

In contrast to this, xenoliths found associated with the pyroclastic rocks on Green Mountain are medium-grained syenites which may have formed relatively high-level plutons beneath Green Mountain. In addition, a block-welded ash-flow tuff was found in these pyroclastics. This indicates that subaerial volcanic rocks are present beneath Green Mountain and also that the history of felsic volcanism on the island is older than indicated by the

present surface geology.

### 3.3.6 Sediments and sedimentary rocks

Sediments are very limited on Ascension both because of the young age of the island's volcanic rocks and the low rainfall. The most abundant sediments are alluvial fan deposits, which are unconsolidated and poorly sorted, and consist of trachyte pumice, basaltic ash, and minor lava flow clasts. The alluvial fans merge with sand and gravel in dry stream channels.

Extensive, flat-lying beds of tuffaceous sandstone, siltstone and mudstone with minor conglomerate are exposed around the east end of Cricket Valley. These deposits, here named the Cricket Valley sediments, are about a square mile in area. They were deposited in standing water, which would indicate that a large closed basin was present.

A small closed basin formed at the Devil's Riding School due to central subsidence of trachyte. Airfall beds of trachyte pumice lapilli and basaltic ash filled the depression. Further subsidence downwarped these beds, and ponded water altered some ash layers to clay. Erosion of the tilted beds around the edge of the basin has produced the notable concentric outcrop pattern.

The beach sands and a few lithified beach exposures are bioclastic sands and therefore the only non-volcanic material on Ascension Island. The white to light yellow coarse sand is formed by wave action breaking up and rounding sea shells and corals. Similar sand deposits have, no doubt, been buried by ash and lava flows and may therefore constitute a small part of the island's subsurface.

### 3.3.7 Structural geology

Structures such as faults and fractures often form the fluid pathways of

geothermal systems. These structures bring fluids into an area in the crust where they can be warmed by the heat source, form a reservoir in which the fluids may reside, or convey heated fluids toward the surface. As fluids migrate along these pathways and begin to heat, they chemically and physically alter the rocks through which they pass. Alteration often decreases the permeability of these rocks and tectonic fracturing is required to keep these pathways open.

Structures also control the locations of volcanic vent areas. In many parts of the world young vent areas, and the structures along which they reside, are the hosts for geothermal reservoirs. The following sections of this report describe structures which were defined by our field work on Ascension Island. The structural features which will be discussed have been compiled on Figure 3-11.

#### 3.3.7.1 Vents, explosion and subsidence features

Both central vents and fissure vents have been active on Ascension Island. Most of the cinder cones appear to have formed around a single active vent although a few, such as Command Hill and Street Crater (Plate I), had two or three vents. Fissure eruptions forming spatter cones and lava flows have occurred on Letterbox, the south side of Sisters Peak, and Booby Hill extending to south of Gannet Hill. Fissure vents are located where a dike reaches the surface and all these vents occur along major structural zones.

All felsic rocks on Ascension have been erupted from central vents. A major, relatively old trachyte vent is evident at the east end of Green Mountain (Fig. 3-11, Plate I). This is probably the source of the extensive trachyte flow which underlies Middleton Peak and is exposed north of Monkey Rock. The structural importance of the Green Mountain trachyte vent is

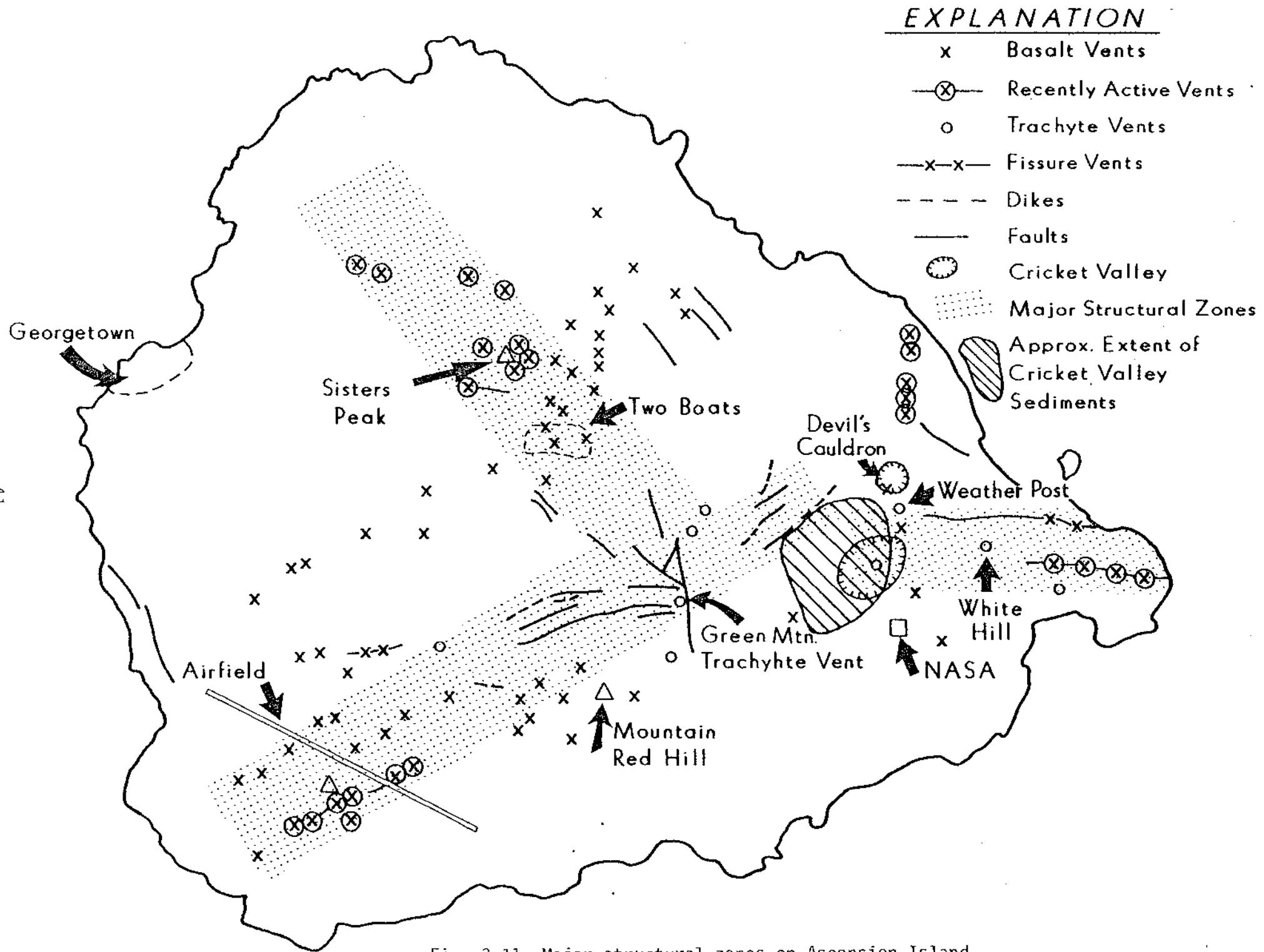


Fig. 3-11 Major structural zones on Ascension Island.

indicated by fault zones which radiate from the vent and are discussed below.

The more recently active trachyte vents are located on the east end of the island. The combination of rapid buildup of volcanic gases and the viscous nature of the trachyte lavas has resulted in explosions which have excavated Devil's Cauldron.

Withdrawal of magma from a near-surface magma chamber probably resulted in the subsidence which formed Cricket Valley. Similar subsidence, but on a much larger scale, may have produced the closed basin in which the extensive Cricket Valley sediments, discussed earlier, were deposited. The evidence suggests that a closed depression with an area of about  $2 \text{ km}^2$  formed at an elevation of 520 m probably as a result of cauldron subsidence over a shallow magma chamber. Deep erosion to the east and northeast has exposed mostly trachyte making up this portion of Ascension Island.

#### 3.3.7.2 Faults and structural trends

Faults, dikes, fissure vents and aligned vents combine to define three major structural zones on the island (Fig. 3-11). From the east end of the island fissure vents, a fault and a dike trend west to White Hill and Weather Post. From the Green Mountain trachyte vent, faults and major basalt vents define an active zone to the northwest (N44 to 51°W), and faults, dikes and vents extending southwest (S57 to 78°W) from Green Mountain define the third structural zone (Fig. 3-11). All but one of the youngest basaltic vent areas occur along these zones. Note also that these zones divide the island into thirds, a pattern similar to that found in the Hawaiian Islands.

Two secondary north-south structural trends are defined by alignment of basalt vents from Sisters Red Hill to Traveller's Hill and from Hummock Point through Devil's Cauldron to the east end of Cricket Valley.



### 3.3.8 Thoughts on the eruption history of central and eastern Ascension Island.

Central and eastern Ascension Island are the areas of youngest and most voluminous outpouring of trachytic magma. Through the limited amount of radiometric dating which has been completed (Section 3.3.11) and the field relationships which have been documented on Plate I we can present some initial arguments concerning the history of development of this area of most complex geology.

Erosion has cut deep enough on the central and eastern part of Ascension to allow some of the relative ages of rock units to be determined. Below Powers Peak, in the Spire Beach area, minor basalt flows and ash are interbedded with the dominant trachyte flows, domes and pyroclastics. These rocks are probably among the oldest units exposed on the island and are part of the volcanic edifice in which the Cricket Valley sediments formed. This volcanic edifice is here referred to as the Cricket Valley sediments caldera to distinguish it from the current Cricket Valley depression which is a much younger subsidence feature.

A maximum age can be estimated for the formation of the Cricket Valley sediments caldera based on stratigraphic exposures. The Middleton Ridge rhyolite flow has been dated at  $0.94 \pm 0.19$  m.y. (Table 3-11, sample AS-2). The two rhyolite lava flow exposures north of Monkey Rock (north slope of Green Mountain) occur at the same elevation and have the same outcrop characteristics as the Middleton Ridge flow and are assumed to be part of the same flow. On Middleton Ridge and north of the Monkey Rock the rhyolite flow is overlain by trachyte flow breccia and pumice lapilli. Northeast of Monkey Rock the Middleton Ridge rhyolite lava flow is also overlain by a distinctive

andesite lava flow (af on Plate I, sample AS-9). To the east the andesite flow is overlain by basaltic cinders that are overlain by an intra-caldera basalt flow in turn overlain by the Cricket Valley sediments (Plate I). The Cricket Valley sediments and caldera are, therefore, younger than the Middleton Ridge rhyolite and less than a million years old. This age relationship can also be demonstrated by a second set of exposures directly east of Monkey Rock. In this area the Middleton Ridge rhyolite is overlain by a trachyte pumice unit which is overlain by a basaltic ash in turn overlain by another trachyte pumice unit and a trachyte dome (Plate I and Plate II, CC'). The uppermost trachyte pumice and dome have been cut off to the southeast by part of the ring fracture system of the Cricket Valley sediments caldera.

Overlying the Middleton Ridge rhyolite flow is the eruptive complex associated with the Green Mountain trachyte vent (Fig. 3-10, Plate I). This volcanic complex consists of a thick and wide-spread trachyte pumice lapilli and volcanic breccia unit with interbedded basaltic ash. It forms the upper part of Middleton Ridge, Hospital Hill, the ridge along the Green Mountain road and the area around the Residency. Within the vent, which is directly south of Lion House, a columnar-jointed dacite lava flow (sample AS-11) overlies the pumice unit and the vent is capped by a trachyte dome. The next to last eruption from this vent formed a trachyte lava flow on the south side, probably contemporaneous with dome formation. After a thin tuff was deposited, a dacite lava flow (sample AI-82-24) erupted over the first lava flow on the south flank. The age of the Green Mountain trachyte vent relative to the Cricket Valley sediments caldera is uncertain but they appear to be roughly contemporaneous.

After the Cricket Valley sediments had been deposited, volcanic breccia, probably from the Weather Post, was spread over the sediments. This volcanic breccia consists of trachyte and basalt rubble. It thickens toward Weather Post and caps the ridge north of Cricket Valley. About this same time the large trachyte lava flow which extends to North East Point was extruded from a vent in the Weather Post-Devil's Cauldron area. The lava flow was followed by eruption of pumice lapilli and the Weather Post dome.

The Green Mountain basaltic cinder cone overlies the Green Mountain trachyte vent to the west and the Weather Post volcanic breccia to the east. The age of the Green Mountain cinder cone relative to the Weather Post dome is uncertain, however. After emplacement of the volcanic breccia, and the eruptions of Weather Post dome and the Green Mountain cinder cone, Cricket Valley subsided. Subsidence of Cricket Valley was probably associated with a nearby trachyte eruption, but which one is uncertain.

Eruption of the small trachyte flow from the Devil's Cauldron vent was followed directly by explosive formation of Devil's Cauldron. A volcanic flow breccia (tv, Plate I), probably erupted from Devil's Cauldron during its formation, caps Weather Post and the Devil's Cauldron trachyte flow (Plate I) and may be the youngest trachyte unit on Ascension. An attempt was made to date the Devil's Cauldron lava flow (Sample AI-82-13, Table 3-11 and Plate III), however, the sample contained no detectable radiogenic argon, suggesting that it is very young. White Hill trachyte dome is also rather young based on the limited extent of weathering and erosion.

After formation of Devil's Cauldron and a similar small explosion crater on the south side of the Weather Post dome, small basaltic or possibly andesitic lava flows issued from vents on the sides of Weather Post, one

flowing into Cricket Valley and the other into Devil's Cauldron (Plate I).

### 3.3.9 Alteration

When geothermal fluids pass through rocks the minerals of the rocks are often altered. These zones of alteration are useful for determining the locations of geothermal activity and identifying the structures which have controlled the hot fluids.

The only area where extensive alteration is exposed on the island is along the Green Mountain Road just below the Red Lion. In this area several faults cut trachyte pumice and the Green Mountain trachyte dome. The rocks are weakly to strongly argillized with moderate hematite staining along structures. The alteration seems to occur along the north rim of the trachyte vent and similar alteration is exposed along faults on the south rim, at the base of the dome. Small areas of hematite staining and moderate clay alteration are also exposed along the southwest trending faults on the southwest-trending side of Middleton Ridge.

### 3.3.10 Hydrology

Water beneath the surface of Ascension Island will either be ocean water from infiltration from the surrounding Atlantic or fresh water derived from rain and condensation. Geothermal systems require water to transfer heat toward the surface where it can be intersected at reasonable drilling depths.

Climatic conditions at Ascension AAF are summarized in Table 3-9 which was provided by Major R. C. Parker of the Staff Meteorology Section at Patrick AFB. The weather station is located at an elevation of 264 feet above sea level. Table 3-9 is included in this report to document the amount of meteoric water potentially available for recharge of a geothermal system and to provide information that is often needed for project planning. Rainfall

TABLE 3-9 Climatology for Ascension Island AAFB

Prepared July 1976

Period of Record: Sept 1942 - Dec 1946. Feb - Apr 1947. Sept 1957 - Jan 1967

PARAMETER	JAN	FEB	MAR	APR	MAY	JUN	JUL	AUG	SEP	OCT	NOV	DEC	ANNUAL TOTAL
<u>Wind (mph)</u>													
Prevailing	ESE 15	ESE 15	ESE 15	ESE 17	ESE 17	ESE 17	ESE 17	ESE 16	ESE 15	ESE 15	ESE 15	ESE 15	ESE 16
Peak Wind	ESE 30	ESE 33	SE 30	ESE 32	SE 36	ESE 33	ESE 33	SSE 31	ESE 35	ESE 30	SE 30	ESE 30	SE 36
<u>Temperatures (°F)</u>													
Extreme Max.	89	89	89	90	89	87	87	84	84	84	86	87	90
Mean Max.	83	85	86	86	84	82	81	80	79	79	80	83	82
Mean	78	80	81	81	80	78	76	75	74	75	76	77	77
Mean Min.	73	75	76	76	75	73	72	70	70	70	76	72	72
Extreme Min.	66	68	70	69	67	67	67	65	63	65	64	64	63
<u>Relative Humidity</u>													
Mean (%)	74	74	74	72	70	69	69	70	73	74	72	73	72
<u>Precipitation</u>													
Days w/Precip	16	12	14	20	15	19	17	18	21	24	22	19	217
Days w/Precip $\geq$ .005 In.	7	5	7	8	6	8	7	8	10	12	8	8	94
Monthly Max. (in.)	1.41	1.36	11.60	3.94	.90	1.49	1.40	1.31	.93	.86	.78	.52	-----
Monthly Mean (in.)	.33	.36	1.46	1.21	.43	.61	.50	.44	.38	.48	.29	.29	6.78
Monthly Min. (in.)	.07	.01	.07	.05	.01	.05	.18	.02	.12	.10	.03	.09	-----
24 Hour Max. (in.)	.91	1.31	6.68	2.03	.34	.99	.82	.52	.21	.26	.17	.22	-----

Table provided by Staff Meteorology Section, Patrick AFB

47

varies to a great degree over the island with most precipitation falling on Green Mountain and its windward (SE) side. The earlier settlers established catchment basins on Green Mountain and Weather Post to provide their fresh water. The basaltic ash that covers Green Mountain is moist and earlier settlers have also dug shallow wells to accumulate this water. No springs are known on the island although minor seeps of surface water can be found on the upper portions of Green Mountain. Daly (1925, p. 30) reports a "drip" immediately north of the present town of Two Boats. We were not able to find this feature. Periodic heavy rains do soak the island and flash flooding is not unknown.

Much of the moisture received by Ascension Island infiltrates the ground quickly due to the high permeability of the volcanic rocks. Once in the subsurface, the course of the infiltrating groundwater is determined by distribution of impermeable rock types (including dikes), present topography, and paleotopography. The water will infiltrate to a fresh water table that will in a general way mimic the overlying topography. Near the ocean, and possibly under much of the island, this fresh water table will come into contact with and overlies salt water.

Several holes were drilled for fresh water on Ascension Island during World War II. The following description is extracted from a history by 1st Lt. William A. Chapman of the 898th Engineer Aviation Co.

...the War Department sent a water geologist to Ascension Island about September 25, 1943 to determine the possibilities of drilling a well for water. The geologist located three sites where wells might produce water. A civilian concern was given the contract for drilling a test well. This organization was to assist the drillers where necessary. Later the organization took over the supervision of the drilling operations. The well was begun about November 20, 1943. A percussion type drilling outfit was used. The location of the test well was approximately 670 feet above sea level and water was anticipated at sea level. The

method was to drive a steel casing along with the hole and when a strata of rock was encountered drill through it and continue with a smaller size casing. The hole was started with eight inch casing and reduced to six inch casing at the first strata of rock, which occurred at 180 feet. At about 270 feet another strata of rock was encountered. The minimum size casing on hand was four inch and as it would not be practicable to reduce to this smallest size at such a shallow depth, the rock was reamed out and the six inch casing continued. Three strata of rock were penetrated in this manner. At about 370 feet the six inch casing had to be stopped. At this depth it would still be impractical to reduce to four inch casing so a method of cementing the inside of the hole was developed to substitute for casing. Considerable difficulty was encountered at the end of the six inch casing. The casing went crooked and the shoe became bent. This necessitated much blasting and cementing and back filling. Finally, the hole was started true again. When the well was about 400 feet deep this organization was returned to the United States and at this time the results of the well are unknown.

During our field studies on Ascension we found two well locations (Plate III). It was our intention to sample any water in these wells and log temperature gradients. Since no location is given in Lt. Chapman's report, there was no way of determining which of the two locations he was describing. The well location to the northeast of Two Boats is easily found because the drilling tower is still in place above the hole. However, the hole is blocked with debris and efforts to clean it out were unsuccessful. The second location (GH-1 on Plate III), consisting of two wells, is located on the alluvial flats southwest of Hospital Hill. The deepest of these is open to about 111 feet. There is no standing water in the well, but material adhering to our probe suggests that the walls of the hole are composed of moist volcanic alluvium. The bottom hole temperature measured in this hole was 1.4°C above the surface temperature.

### 3.3.11 Geochronology

As has been discussed previously in this report, the age of volcanic rocks is used in the exploration for geothermal resources as an indication of potential heat sources. The volcanoes of Ascension Island have certainly been

active in historic time, although if this activity was observed by man it was not recorded. The island was discovered by Portuguese Admiral Joao de Nova Gallege on 20 May, 1501. The island was settled on a permanent basis in 1815 and thus we know that there has been no volcanic activity since that time. However, the descriptions of the island prior to 1815 are not detailed enough to allow the conclusion that there had not been volcanic activity between 1501 and 1815.

The unweathered nature of the flows which have emanated from the Sisters Peak and South Gannet Hill areas suggests that these flows are several hundred years old. Basalts that are this young are difficult to date by radiometric methods. Thus we attempted to find material which would produce young dates in a geologic position such that it would give us a maximum or minimum age for these young flows.

Sample AS-12 of bioclastic beach sand was collected from beneath a basaltic ash layer 1300 m south of English Bay. The paleobeach sand onlaps against an older basalt flow to the east. The basalt shows no evidence of wave erosion. The black airfall basaltic ash above the bioclastic sand is 30 to 60 cm thick and is overlain to the west by the young Sisters Peak basalt flow. The sand is unconsolidated at the top but is weakly cemented 1.5 m below its upper contact. The sand is fine grained (0.1 - 0.3 mm), subrounded to subangular and contains about 7 percent volcanic grains. Present beach sand is coarse grained, rounded and contains only 2 percent volcanic grains. The finer grain size of the buried sand suggests that it may be wind deposited. The bioclastic grains consist mostly of aragonite shell fragments and some grains of coral. Original textures are evident in most grains and recrystallization was not detectable. Secondary calcite cement forms about 5



to 10 percent of the rock in lithified samples.

The radiocarbon data for this sample is listed in Table 3-10. It shows that the age of the sand is  $21,850 \pm 500$  years. Thus the beach sand is probably much older than the basalt from the Sisters Peak vent and doesn't give us any more information on the age of the young basalt flows.

Table 3-10 Radiocarbon data for samples of bioclastic beach sand

<u>SAMPLE</u>	<u><math>-\delta C^{14}</math></u>	<u>Age in Years</u>
AS-12	$934 \pm 4$	$21,850 \pm 500$

Five samples of rocks from Ascension Island were dated by the potassium-argon (K-Ar) method. The results of this dating are shown in Table 3-11, and the location of the samples dated are shown in Plate III. The samples were analyzed in the isotope laboratory of the Department of Geology and Geophysics at the University of Utah, by Dr. Stanley H. Evans, Jr. The laboratory procedure is documented in Evans (1980).

Previous dating by Bell et al. (1972) suggests a maximum age determination of about 1.5 million years. However, the location of their sample is unknown.

Most of our dating concentrated on the felsic rocks because of their high potassium content and resultant greater precision for young rocks. Sample AS-2 was collected for dating because of its position at the bottom of the exposed stratigraphic sequence established for Green Mountain. The K-Ar date of this rock unit (Table 3-11) is  $940,000 \pm 190,000$  years. The next youngest rocks analyzed were samples from the Craigs (AI-82-29) at  $740,000 \pm 170,000$  years. As has been stated previously, Bears Back covers an intrusive dome,

Table 3-11 K-Ar data for samples from Ascension Island

Sample No.	Material Dated	Weight (gms.)	%K	Moles/gm		Age (m.y.) $\pm 1\sigma$
				Ar <sup>40</sup> <sub>Rad</sub> (X10 <sup>-11</sup> )	%Ar <sup>40</sup> <sub>atm</sub>	
AS-2	Whole Rock	1.01716	3.84	0.627	93	0.94 $\pm$ 0.19
AI-82-13	Anorthoclase	0.70031	5.40	No detectable radiogenic argon		
AI-82-15	Whole Rock	1.05185	3.51	0.370	97	0.61 $\pm$ 0.28
AI-82-26	Whole Rock	2.03944	1.08	0.025	99.96	0.01 + 0.35 -0.01
AI-82-29	Whole Rock	0.70857	4.25	0.546	94	0.74 $\pm$ 0.17

52

Constants Used:

$$\lambda_{\beta} = 4.962 \times 10^{-10}/\text{yr.}$$

$$\lambda_{\epsilon} = 0.581 \times 10^{-10}/\text{yr.}$$

$$K^{40}/K_{\text{Tot.}} = 1.167 \times 10^{-4} \text{ Mole/Mole}$$

S. H. Evans, Jr., analyst

portions of which are exposed on the south side of the structure. This dome (AI-82-15) was apparently emplaced  $610,000 \pm 280,000$  years ago. When these three dates are plotted with their error bars (Fig. 3-12), it is seen that within the limits of error all could have been emplaced at about the same time. However, geologic evidence shows that the rhyolite flow (AS-2) is at least older than the Bears Back dome.

Sample AI-82-26 was collected from the older basalt flow along the Old Mountain Road. The sample dates at 10,000 years, but the error (Table 3-11) is larger than the date. This sample is too young to be dated with certainty by the K-Ar method. Thus we recommend that the date not be used.

Sample AI-82-13 was collected from the flow that vented at Devil's Cauldron. Following the eruption of this flow the Devil's Cauldron feature was formed by an explosion which deposited a blanket of volcanic breccia over the flow. Attempts to date the flow were not successful. No radiogenic argon was detected, indicating that the flow is too young to date by K-Ar methods.

In summary, radiometric dating of rocks from Ascension Island has shown that even the oldest felsic units exposed are less than one million years old. In addition, Devil's Cauldron is one of the youngest felsic volcanic features on the island, and it is too young to be dated by K-Ar method. This evidence all supports the possibility of a granitic melt or partial melt within several kilometers of the surface. This high-level felsic pluton would provide an excellent source of heat for a high-temperature geothermal system.

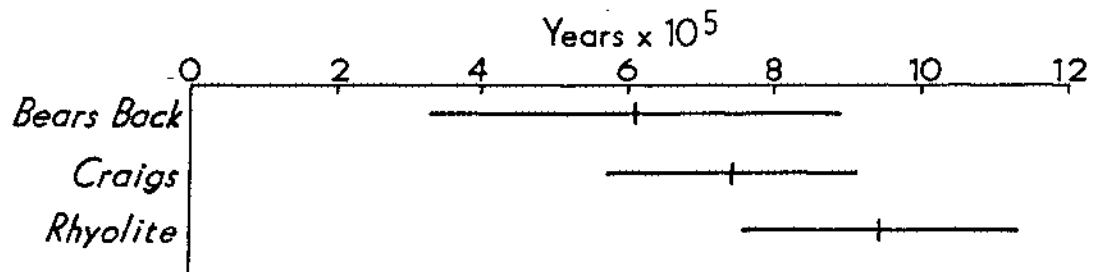


Fig. 3-12 K-Ar dates for three felsic units from Ascension Island. Bears Back sample is AI-82-15, Craigs sample is AI-82-29, and the rhyolite sample is number AS-2.

## 4.0 GEOCHEMICAL SURVEYS

### 4.1 Introduction

In many areas of the world radon and soil mercury geochemical surveys have proven to be cost-effective aids in the exploration for geothermal resources. However, both methods must be used with caution since they will not necessarily work in every environment. In order to test the methods on Ascension, three traverses were made to sample both radon and soil mercury across recognized faults and fractures. These surveys are described in this section, but first we will briefly discuss the theory behind the use of radon and soil mercury surveys in geothermal exploration.

The use of radon geochemistry has been reviewed by Nielson (1978).  $Rn^{222}$  is the longest lived radon isotope and has commonly been used as a geologic tracer. This isotope is a product of the  $U^{238}$  decay series and is present in some amount in all geologic systems. Radon flux in geothermal systems can be evaluated in terms of: 1) the formation of radon by disintegration of parent material and the release of radon from the crystalline structure, and 2) the movement of radon through diffusion and transport processes.  $Rn^{222}$  originates from the decay of  $Ra^{226}$  which emits an alpha particle. The recoil energy of the newly formed  $Rn^{222}$  is sufficient to transport the atom 0.03-0.04  $\mu m$  in rocks. This is the principal method of release of Rn from the rock matrix. It has been found that the amount of radon contributed to geofluids is inversely proportional to the particle size and the flux is thus increased in areas of fracturing.

Because of the short half-life of  $Rn^{222}$  and slow rates of diffusion, a transport mechanism must predominate if radon is to migrate appreciable distances. In the near-surface environment, transport processes are dependent

on atmospheric variables including barometric pressure, wind velocities, and precipitation. These factors are very difficult to quantify but they can be compensated for by integrating the radon flux over time. This method, coupled with a structural analysis, can be useful as a site-specific exploration tool, particularly in locating exploration holes in known geothermal areas.

The use of soil mercury geochemical surveys for geothermal exploration has been met with wide acceptance (Capuano and Bamford, 1978). In contrast with radon, which is generated along structural zones, mercury vapor is produced at the boiling interface of a geothermal system. Mercury is partitioned into the vapor phase along with sulfur species and  $\text{CO}_2$ . Once in the vapor phase, it ascends to the surface and is generally concentrated in the near-surface environment by adsorption on clays and organic material. In this context it defines permeable zones which connect the active geothermal system with the surface. Care must be taken that samples are not contaminated by pre-existing Hg concentrations.

#### 4.2 Surveys

Soil samples were collected along three traverses that crossed mapped faults and fractures. The uppermost 2" of soil were removed and the samples were taken 2-6" beneath the surface. Then samples were placed in plastic bags and numbered with the number of the radon cup which was placed in the hole. In the laboratory, the soil samples were dried and sieved. The -80 mesh fraction was used for the Hg analysis. The analyses were performed using a Jerome Instruments gold-film mercury detector. The detection limit on this device is 5 ppb Hg.

In order to integrate the radon flux over time, Track-Etch detectors manufactured by the Terradex Corp. were placed in the ground. The holes were

about one foot deep. The cups were placed in the ground on 7/26/82 and 7/27/82 and were retrieved on 8/24/82. The results have been normalized to a 30 day exposure.

The surveys were run in three different parts of the island with two of the surveys sampling areas of basaltic rocks and one over an area which is underlain by trachytic pumice. The survey locations are shown in Plate 3. The results of the Rn and Hg surveys are shown graphically in Figs. 4-1, 4-2, and 4-3. In addition to the soil surveys, a mercury traverse was run across an alteration zone exposed at the last switchback before the pig pens on the road up Green Mountain. These zones are clearly controlled by fractures cutting the trachytic pumice sequence. In addition, samples were collected in the unaltered pumice for background. None of the samples collected contained Hg above the detection limits of 5 ppb.

In the case of the three traverses (Figs. 4-1, 4-2, and 4-3), the Hg values were commonly below detection limits of 5 ppb. Thus no statistics have been calculated for the survey values. Statistics for the radon survey are shown in Table 4-1.

Table 4-1 Statistics of Radon Track Etch Surveys

<u>Survey</u>	<u>No. of Samples</u>	<u>Mean</u>	<u>S.D.</u>
AI-Sis	35	11.7	3.6
AI-Pumice	25	208.8	116.5
AI-Donkey	40	50.6	28.0
All Surveys	100	18.3	10.4

Table 4-1 shows the importance of rock type on survey results. The AI-Sis survey was run on the young basalt cinders to the northwest of Sisters Peak. These rocks are undoubtedly low in uranium and are young enough that the uranium which is present certainly has not established equilibrium with its

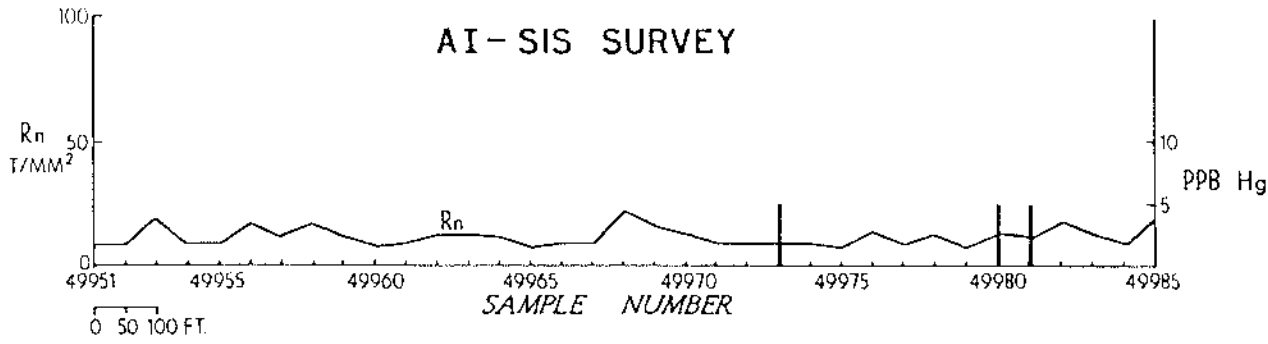


Fig. 4-1 Radon and mercury survey results for AI-Sis survey. Survey location is shown on Plate III.

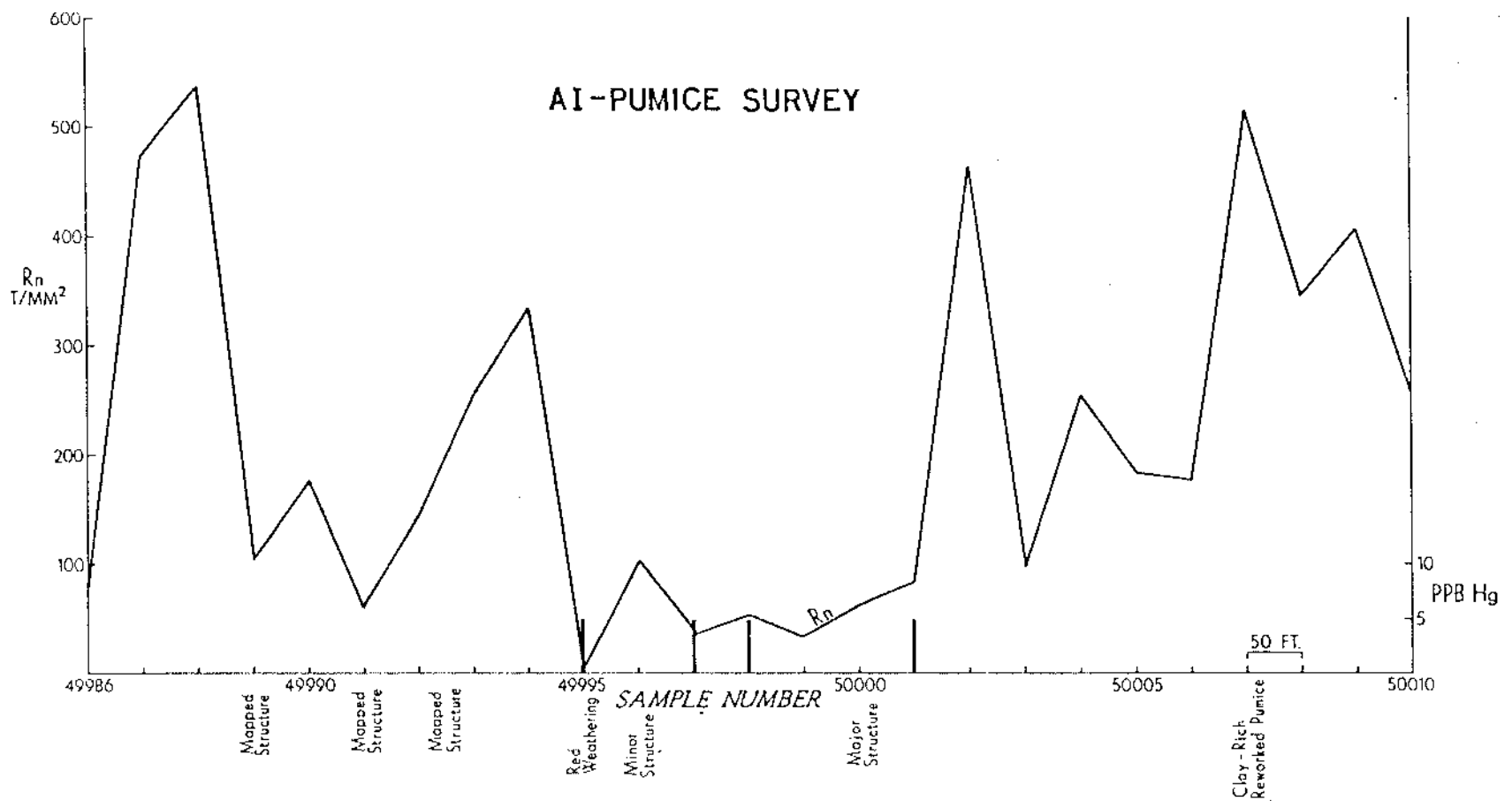


Fig. 4-2 Radon and mercury survey results for the AI-Pumice survey. Survey location is shown on Plate III.



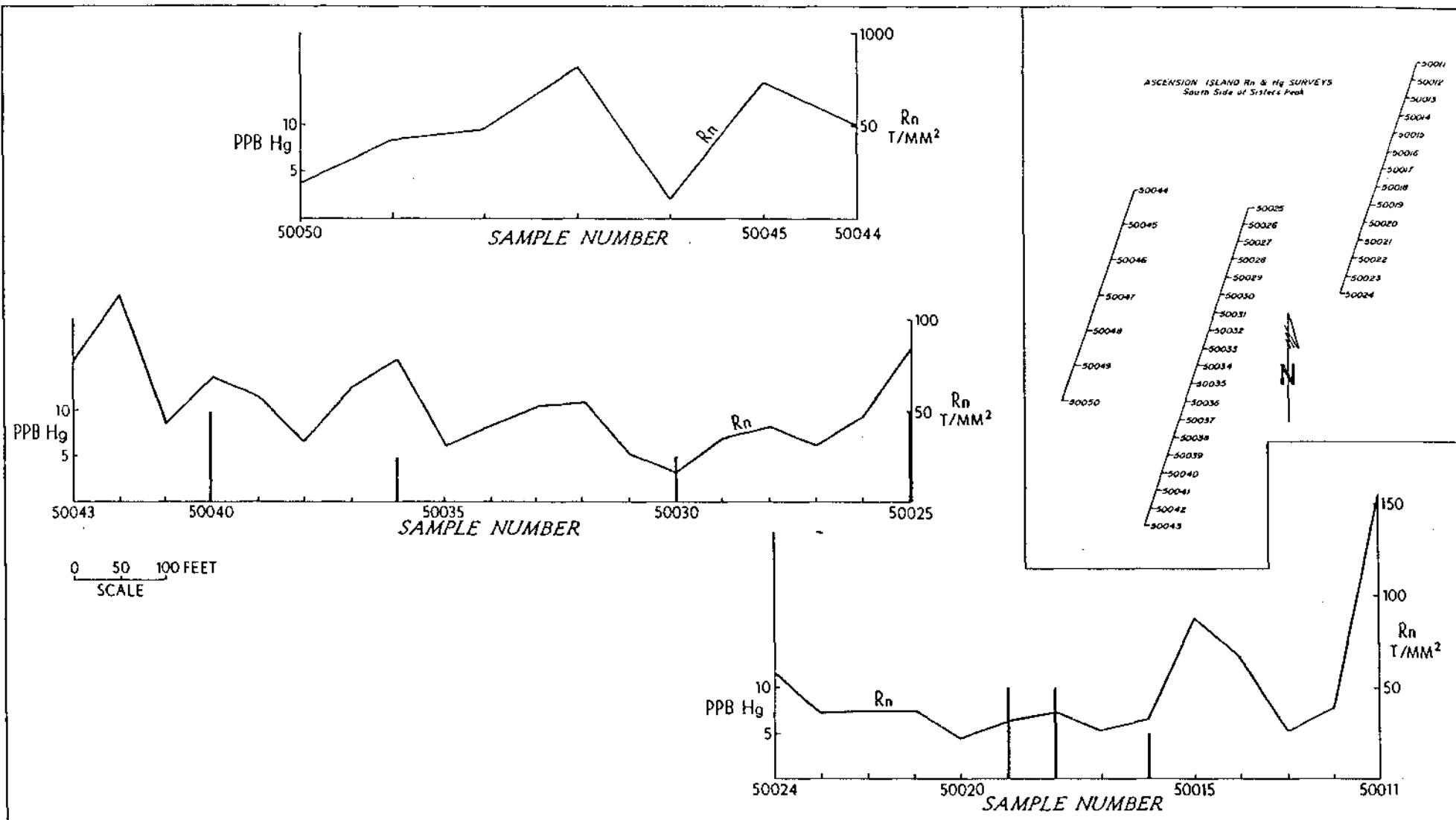


Fig. 4-3 Radon and mercury results for AI-Donkey survey. Survey location is shown on Plate III. Insert maps survey sample locations.

daughter products. The AI-Donkey survey was run over older rocks as well as fine-grain sedimentary material which probably includes the weathered products of trachyte pumice and crystalline rocks. It can be seen from Table 4-1 that the resultant mean and standard deviation about the mean are higher than in the AI-Sis survey. The highest mean values were obtained from the AI-Pumice survey which was run over an area underlain by trachyte pumice. This is predictable in consideration of both the age of the unit and the relatively high uranium content of the rock.

The purpose of the Rn survey was to locate structures which may control dike emplacement and/or the ascent of geothermal fluids. Theoretically a structure which controls geothermal fluids should show up as both a radon and a mercury anomaly. To test the method on Ascension, the AI-Sis and AI-Pumice surveys were run over areas where structures had been recognized. The AI-Sis (Fig. 4-1) survey does not show appreciable variation along its entire length. The AI-Pumice survey (Fig. 4-2), on the other hand, shows extreme variation but generally shows lows along areas where faults and fractures were recognized at the surface. This result is probably due to the sealing of these fault and fracture zones by precipitation of silica. There is no evidence that this silica was related to a hydrothermal system but rather is probably derived from the devitrification of adjacent silicic ash and pumice.

It is concluded from the Hg and Rn analysis that the methods would be difficult to use on Ascension. Lack of soil and vegetation development have resulted in the low clay and organic content of the soils thus eliminating the principal concentration mechanisms of mercury. Because of the youth of the rocks and the relatively low uranium content of the basalts, fracture zones do not show up well above the background of the survey. In addition, sealing of

fracture and fault zones by silica deposition in the near surface may falsely steer exploration away from potentially important fracture zones. Thus, we conclude that Hg and Rn soil surveys should not be used for geothermal exploration on Ascension without proper justification. This conclusion in no way bears on the applicability of subsurface trace element zonation which must await the completion of drill holes for assessment.

## 5.0 PHASE I CONCLUSIONS

The geologic work done on Ascension Island during the Preliminary Examination Phase of this project has demonstrated that there is a very high potential for the discovery of a geothermal resource. In fact, it is our opinion that Ascension Island has one of the highest geothermal resource potentials of any unexplored area in the world today. We base this conclusion on the young age of the volcanic activity observed on Ascension Island which provides a heat source, on the consideration that fluids to transport heat exist, and that geologic structures, which provide permeability, are common.

We recommend that the U. S. Air Force proceed with Phase II of this project, the geothermal exploration of Ascension Island. This exploration program must be implemented in order to locate and evaluate a geothermal resource. The strategy of this exploration program is outlined in detail in the following section.

## 6.0 PHASE II EXPLORATION STRATEGY

The exploration strategy to be followed in Phase II is outlined in Figure 6-1. The strategy is derived from the facts that we have learned about Ascension during Phase I and our geothermal exploration experience. The strategy employs less expensive methods to ensure the proper placement of the thermal gradient holes, the most expensive portion of the Phase II effort.

The Phase II effort will start with the activities shown in boxes 5 through 7 on Figure 6-1. First, we will talk with the Royal Air Force about any thermal IR anomalies they may have detected in the sea around the island with their NIMROD aircraft. It may be possible that submarine emanations of thermal fluids exist and can be detected by the equipment aboard these aircraft. Next (Box 6) we will request that the RAF contribute the use of one of the helicopters stationed at Ascension to fly an aeromagnetic survey of the island. It is estimated that this survey would require about two days of flying which could be interspersed with the helicopter's regular duties. For this participation, we will offer the RAF copies of our compiled aeromagnetic map and report. The aeromagnetic data will be extremely useful in delineating subsurface structure by mapping magnetic contrasts between adjacent rock units.

During the initial field work on Phase II, we will also run a resistivity orientation survey (Box 7) to test the applicability of the resistivity method on Ascension Island. Resistivity surveys are very valuable in other geothermal areas because they delineate high electrical conductivity zones at depth which are produced by hot geothermal fluids and by alteration of rock masses traversed by these fluids. We are concerned that these methods may not work on Ascension because the high resistivity of the surface layers may

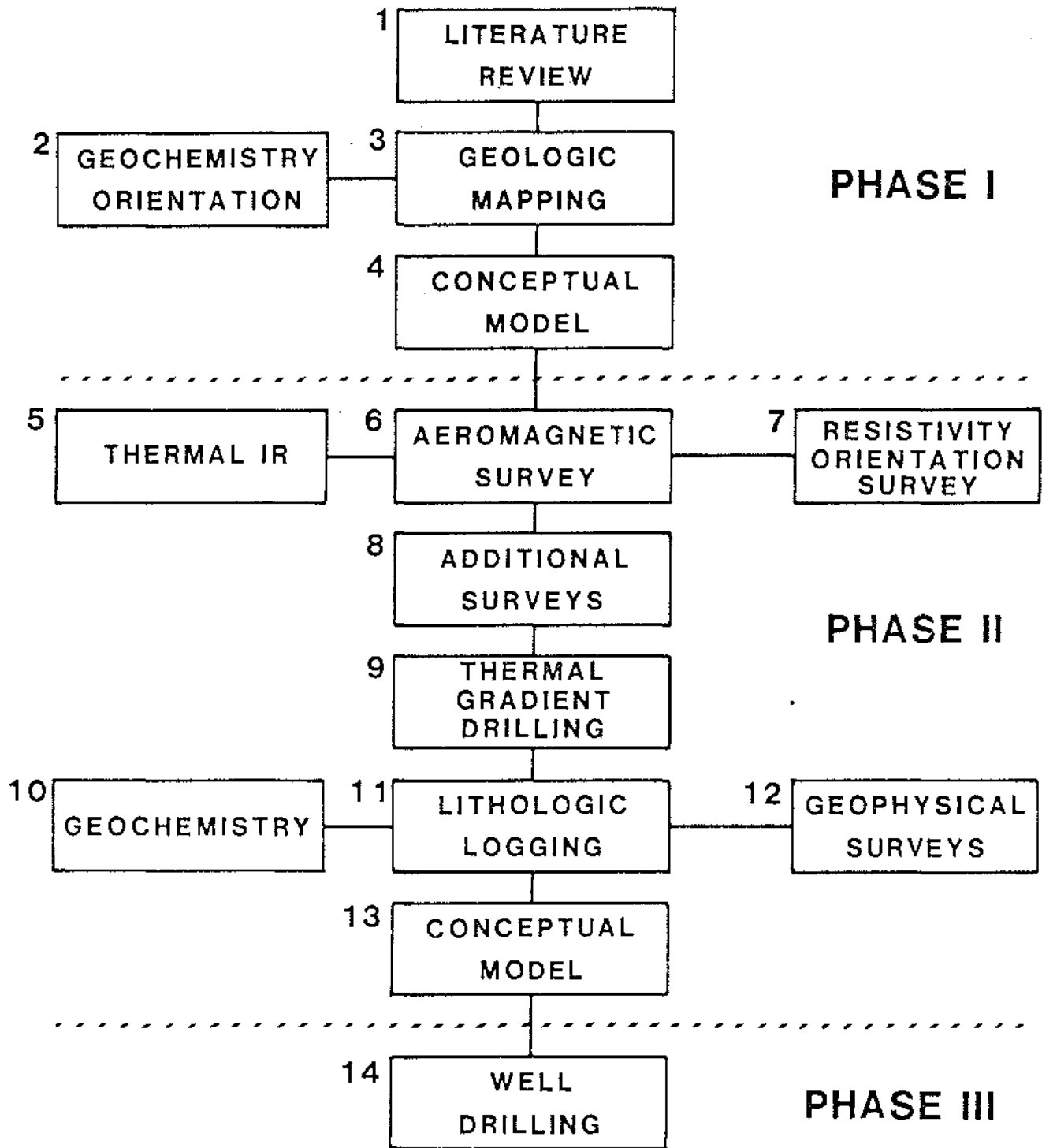


Fig. 6-1 Phase II exploration strategy.

inhibit our ability to get the required electrical current into the ground. In addition, interference from the electronic complexes on the island may completely mask our signals. If we can demonstrate that a resistivity survey could be useful, we would return to the island with a crew prepared to run that survey (Box 8).

The above surveys are all designed to outline the areas with the highest geothermal potential. These areas will then be the sites for drilling small diameter holes principally for the measurement of thermal gradients (Box 9). In addition, these holes will be logged by geological, geophysical, and geochemical methods to gain as much information as possible about the surface of Ascension Island (Boxes 10, 11, 12). In order to drill these holes we will have to mobilize a drilling rig and support equipment to Ascension. Representatives of ESL have already spoken with the PAN AM manager on the island about the availability of equipment and personnel to help with this portion of the project. In order to minimize transportation costs, we will ship as much equipment as possible by boat.

Following the completion of the thermal gradient and associated studies, we will update our conceptual models of the system at Ascension (Box 13). The above work will also provide the information necessary to recommend termination of the project or continuation into Phase III, the drilling of a geothermal test well.

## 7.0 VOLCANIC HAZARDS

The volcanoes of Ascension are currently dormant, but the likelihood of renewed activity in the future is high. Volcanic centers typically are dormant for hundreds to thousands of years between periods of eruptive activity, which last a few years. When discussing volcanic hazards on Ascension it should be remembered that the next eruption may not occur for hundreds or thousands of years and the probability of an imminent eruption is not great.

A few predictions can be made about the possible nature and effects of an eruption. Warning signs such as small but frequent earthquakes and steaming ground or fumarolic activity will probably precede an eruption by weeks or months. The most likely type of eruption would produce basalt ash, cinders, and lava flows. The volcanic ash would be dispersed downwind from the vent, and would reduce visibility, make breathing difficult, and clog air filters on motors. Lightning generated by the ash fall could disrupt electronic communications and damage equipment. However, a basaltic eruption would probably not be violent enough or widespread enough to require evacuation of the island. Only the immediate area around the active vent and the downwind area would be significantly affected.

A more felsic eruption, although less likely to occur, would be much more violent. An eruption such as the one that produced the Devil's Cauldron could include massive explosions and pumice lapilli or ash falls affecting the entire island.

No preparations for possible volcanic activity are recommended at this time because of the very low probability of an imminent eruption and the inability to predict the location of an eruption.



The prediction of volcanic events is a non-precise science at best. By documenting the dates of previous eruptions and the time between eruptions, some evidence may be gained as to the timing of potential future eruptions. Some of this information will undoubtedly be generated during our geothermal program, and we will endeavor to keep the USAF informed of its significance. In addition, monitoring of seismic noise on Ascension could greatly increase the precision of predicting the onset of an eruption.

## 8.0 ACKNOWLEDGEMENTS

We would like to acknowledge the cooperation and enthusiasm of a number of people and organizations who contributed to the smooth completion of this project. These include George Hotchco, Lt. Col. William D. Bryden, and Lt. Col. Ed Roscoe of the U.S. Air Force as well as William Koslow of Pan American World Services and Don Coffee, PAN AM Manager, and his staff on Ascension Island.

## 9.0 REFERENCES CITED AND ASCENSION BIBLIOGRAPHY

- Atkins, F. B., Baker, P. E., Bell, J. D., and Smith, D. G. W., 1964, Oxford expedition to Ascension Island: *Nature*, v. 204, no. 4960, p. 722-724.
- Baker, P. E., 1973, Islands of the South Atlantic, in *The Ocean basins and margins*, vol. 1, The South Atlantic, Plenum Press, New York, p. 493-553.
- Baker, P. E., 1975, Peralkaline acid volcanic rocks of oceanic islands: *Bull. Volcanologique*, v. 38, p. 737-754.
- Bell, J. D., 1967, The occurrence of obsidian and other natural glasses on Ascension Island, with discussion: *Geol. Soc. London, Proc.*, no., 1641, p. 179-181.
- Bell, J. D., 1965, Eruption mechanism on Ascension Island: *Proc. Geol. Soc. London*, v. 1626, p. 145-146.
- Bell, J. D., Atkins, F. B., Baker, P. E., and Smith, D. G., 1972, Notes on the petrology and age of Ascension Island, South Atlantic, abst.: *EOS (Am. Geophys. Union, Trans.)*, v. 53, no. 2, p. 168.
- Bleil, U., Hall, J. M., Johnson, H. P., Levi, S., and Schonharting, G., 1982, The natural magnetization of a 3-km section of Icelandic crust: *Jour. Geophys. Res.*, v. 87, B8, p. 6569-6589.
- Brasier, M. D., 1974, Turtle drift, discussion: *Nature*, v. 250, no. 5464, p. 351.
- Cann, J. R., 1967, A second occurrence of dalyite and the petrology of some ejected syenite blocks from Sao Miguel, Azores: *Mineral Mag.*, v. 36, no. 278, p. 227-232.
- Capuano, R. M., and Bamford, R. W., 1978, Initial investigation of soil mercury as an aid to drill site selection in geothermal systems: *Univ. of Utah Res. Inst./Earth Science Lab. Rept. no. 13*, 32 p.
- Carr, A., and Coleman, P. J., 1974, Seafloor spreading theory and the odyssey of the green turtle: *Nature*, v. 249, no. 5453, p. 128-130.
- Christensen, O. D., Kroneman, R. L., Capuano, R. M., 1980, Multi-element analyses of geologic materials by inductively coupled plasma-atomic emission spectroscopy: *Univ. of Utah Res. Inst./Earth Science Lab. Rept. no. 32*, 32 p.
- Cooper, J. A., and Richards, J. R., 1966, Isotopic and alkali measurements from the Vema seamount of the south Atlantic Ocean: *Nature*, v. 210, no. 5042, p. 1245-1246.
- Daly, R. A., 1925, The geology of Ascension Island: *Proc. Am. Acad. Arts and Sci.*, v. 60, no. 1, p. 1-80.

- Darwin, C., 1876, Geological observations on the volcanic islands and parts of South America visited during the voyage of the H.M.S. Beagle: Smith Elder & Co., London, 647 p.
- Dash, B. P., and Milsom, J., 1973, Gravity field of Ascension Island, South Atlantic: *Earth Planetary Sci. Letters*, v. 21, no. 1, p. 79-84.
- Evans, S. H., Jr., 1980, Summary of potassium-argon dating - 1979: DOE/DGE topical report 28392-41, University of Utah, 23 p.
- Ewart, A., 1979, A review of the mineralogy and chemistry of Tertiary - Recent dacitic, latitic, rhyolitic, and related salic volcanic rocks, in Barker, F. (ed.) *Trondhjemites, Dacites and Related Rocks*, Elsevier, Amsterdam, p. 13-121.
- Fleet, S. G., and Cann, J. R., 1967, Vlasovite; a second occurrence and a triclinic to monoclinic inversion: *Mineral Mag.*, v. 36, no. 278, p. 233-241.
- Gast, P. W., Tilton, G. R., and Hedge, C., 1964, Isotopic composition of Pb and Sr from Ascension and Gough Islands: *Science*, v. 145, p. 1181-1185.
- Gast, P. W., 1969, The isotopic composition of lead from St. Helena and Ascension Islands: *Earth Planetary Sci. Letters*, v. 5, no. 5, p. 353-359.
- Heirtzler, J. R., Dickson, G. O., Herron, E. M., Pitman, W. C., and LePichon, X., 1968, Marine magnetic anomalies, geomagnetic field reversals and motions of the ocean floor and continents: *Jour. Geophys. Res.*, v. 73, no. 6, p. 2119-2136.
- King, C. A., 1966, *An introduction to oceanography*: McGraw Hill Book Co., Inc., New York, 337 p.
- MacDonald, G. A., 1968, Composition and origin of Hawaiian lavas: *Geol. Society America Memoir* 116, p. 477-522.
- Mehegan, J. M., Robinson, P. T., and Delaney, J. R., 1982, Secondary mineralization and hydrothermal alteration in the Reydarfjordur drill core, eastern Iceland: *Jour. Geophys. Res.*, v. 87, no. B8, p. 6511-6524.
- Menard, H. W., 1969, Growth of drifting volcanoes: *Jour. Geophys. Res.*, v. 74, p. 4827-2837.
- Mitchell-Thome, R. C., 1970, *Geology of the South Atlantic Islands*: Berlin, Borntraeger, 387 p.
- Moore, J. G., and Fiske, R. S., 1969, Volcanic substructure inferred from dredge samples and ocean-bottom photographs, Hawaii: *Geol. Soc. America Bull.*, v. 80, p. 1191-1202.

- Muecke, G. K., Ade-Hall, J. M., Aumento, F., MacDonald A., Reynolds, P. H., Hyndman, R. D., Quintino, J., Opydke, N., and Lowrie, W., 1974, Deep drilling in an active geothermal area in the Azores: *Nature*, v. 252, no. 5480, p. 281-285.
- Nielson, D. L., 1978, Radon emanometry as a geothermal exploration technique: theory and an example from Roosevelt Hot Springs KGRA, Utah: Univ. of Utah Res. Inst./Earth Science Lab. rept. no. 14, 31 p.
- O'Nions, R. K., Hamilton, P. J., and Evensen, N. M., 1977, Variations in  $^{143}\text{Nd}$  and  $^{87}\text{Sr}/^{86}\text{Sr}$  ratios in oceanic basalts: *Earth Planetary Sci. Letters*, v. 34, no. 1, p. 13-22.
- O'Nions, R. K., and Pankhurst, R. J., 1974, Petrogenetic significance of isotope and trace element variation in volcanic rocks from the Mid-Atlantic: *Jour. Petrol.*, v. 15, pt. 3, p. 603-634.
- Oxburgh, E. R., and Agrell, S. O., 1982, Thermal conductivity and temperature structure of the Reydarfjordur borehole: *Jour. Geophys. Res.*, v. 87, B8, p. 6423-6428.
- Quintino, J., and Machado, F., 1977, Heat flow and the Mid-Atlantic rift volcanism of San Miguel Island, Azores: *Tectonophysics*, v. 41, no. 1-3, p. 173-179.
- Robinson, P. T., Hall, J. M., Christensen, N. I., Gibson, I. C., Fridleifsson, I. B., Schmincke, H., and Schonoharting, G., 1982, The Iceland research drilling project: Synthesis of results and implications for the nature of Icelandic and oceanic crust: *Jour. Geophys. Res.*, v. 87, no. B8, p. 6657-6667.
- Roedder, E., 1970, Laboratory investigations of inclusions in minerals of Ascension Island granitic blocks and their petrologic significance: *Izd. Nauka Moscow (English summary)*, v. 2, p. 247-258 (in Russian).
- Roedder, E., and Coombs, D. S., 1967, Immiscibility in granitic melts indicated by fluid inclusions in ejected granitic blocks from Ascension Island: *Jour. petrology*, v. 8, no. 3, p. 417-451.
- Smith, R. L., and Shaw, H. R., 1975, Igneous-related geothermal system, in Assessment of geothermal resources of the United States, 1975: U. S. Geol. Survey Circ. 726, p. 58-83.
- Stover, C. W., 1968, Seismicity of the South Atlantic Ocean: *Jour. Geophys. Res.*, v. 73, p. 3807-3820.
- Tatsumoto, M., 1969, Comments on paper by P. W. Gast: "The isotopic composition of lead from St. Helena and Ascension islands": *Earth Planetary Sci. Letters*, v. 7, no. 3, p. 224-227.
- Ulyrch, T. J., 1969, A comment on the concordia methods of interpreting whole-rock U/Pb ratios (discussion of paper by P. W. Gast, 1969): *Earth Planetary Sci. Letters*, v. 7, no. 2, p. 116-118.

- van Andel, T. H., 1968, The structure and development of rifted mid-ocean rises: *J. Marine Res.*, v. 26, p. 144-161.
- van Andel, T. H., and Heath, G. R., 1970, Tectonics of the mid-Atlantic Ridge, 6-8° latitude: *Marine Geophys. Research*, v. 1, no. 1, p. 5-36.
- van Andel, T. H., Rea, D. K., von Herzen, R. P., and Hoskins, H., 1973, Ascension Fracture Zone, Ascension Island, and the mid-Atlantic Ridge: *Geol. Soc. America Bull.*, v. 84, p. 1527-1546.
- Van Tassel, R., 1951, Dalyite, a new potassium zirconium silicate from Ascension Island, Atlantic: *Mineral. Magazine*, v. 29, no. 217, p. 850-857.
- Walker, G. P. L., 1960, Zeolite zones and dike distribution in relation to the structure of basalts of eastern Iceland: *J. Geol.*, v. 68, p. 515-528.
- White, D. E., Muffler, L. J. P., and Truesdell, A. H., 1971, Vapor dominated hydrothermal systems compared with hot water systems: *Econ. Geology*, v. 66, p. 75-97.
- White, D. E., and Williams, D. L., eds., 1975, Assessment of geothermal resources of the United States: *U. S. Geol. Survey Circ.* 726, 155 p.

## APPENDIX

### Petrographic Data from Thin Sections

- AI-82-1                      Dacite from the Craigs
- Textures:                      Hiatal porphyritic, 1-3 mm, euhedral orthoclase phenocrysts composing 5% of the rock.
- Matrix texture is panidiomorphic with feldspar laths 0.1 to 0.2 mm long.
- Mineralogic Composition:
- 69% orthoclase (possibly a few plagioclases)
  - 20% orthopyroxene, anhedral (possibly some hornblende)
  - 5% quartz, interstitial
  - 5% opaques
  - 1% apatite
  - Trace zircon
  - Trace allanite
- AI-82-2                      Olivine basalt plug south of Sisters Peak
- Textures:                      Matrix is hyalophitic, trachytic with 0.1 mm euhedral plagioclase laths and anhedral pyroxene, few small vesicles.
- Mineralogic Composition:
- 30% plagioclase
  - 10% pyroxene
  - 60% blackglass (tachylite)
- AI-82-10                      Andesite flow, west side Coconut Bay
- Textures:                      Hiatal porphyritic, granitic-granular. 1-8 mm phenocrysts composing about 38% of the rock.
- Mineralogic composition:
- 25% microcline phenocrysts, subhedral, 4-8 mm. (Some absorption of phenocrysts evident.)
  - 1% plagioclase phenocrysts
  - 5% augite phenocrysts, minor alteration to actinolite and chlorite
  - 7% opaques
  - Trace possible apatite
  - 62% cryptocrystalline matrix with high mafic content

- AI-82-12                      Andesite flow north of Wig Hill, at southeast head
- Textures:                      Vesicular, vitrophyric
- Mineralogic Composition:  
     40% labradorite (optical An 60) euhedral, 1.5 mm  
     5% pyroxene, anhedral, to 0.5 mm  
     55% glass, devitrifying to microlites
- AI-82-13                      Dacite(?), Devil's Cauldron flow
- Textures:                      Vitrophyric, flow-banded, abundant elongate vesicles  
    in glass matrix
- Mineralogic Composition:  
     3% orthoclase, phenocrysts, euhedral, 0.5-2 mm  
     Trace possible plagioclase  
     Trace augite phenocrysts, 0.1-0.2 mm  
     10% feldspar microlites  
     87% glass (patchy alteration to clay)
- AI-82-14                      Basalt flow bf<sub>1</sub>, north of Sisters Peak
- Textures:                      Vesicular, vitrophyric
- Mineralogic Composition:  
     40% andesine, euhedral laths 0.3 mm long, optical An 35  
     7% olivine, anhedral 0.1-0.2 mm  
     53% black glass and opaques
- AI-82-15                      Dacite intrusive dome, Bears Back
- Textures:                      Hiatal porphyritic, trachytic, 3-5 mm subhedral  
    sanidine phenocrysts composing 10% of the rock.  
    Matrix is idiomorphic with 0.1 - 0.3 mm feldspar  
    laths.
- Mineralogic Compositions:  
     75% sanidine, abundant inclusions near the phenocryst edges  
     3-5% quartz, interstitial  
     15% hypersthene, anhedral, matrix mineral  
     5% opaques  
     Trace augite phenocrysts  
     Trace zircon
- AI-82-16                      Andesite, Drip Dome at Two Boats
- Textures:                      Non-porphyritic, irregular vesicles
- Mineralogic Composition:  
     Feldspar laths, 0.1 mm in a matrix of glass and pyroxene.  
     25-30% opaques



- AI-82-18 Basalt flow, uplifted blocks south of Sisters Peak
- Textures: Porphyritic, pilotaxitic, 1-2 mm phenocrysts of euhedral plagioclase, 2%, and olivine, 1% of the rock. Matrix consist of 0.2 mm anhedral crystals
- Mineralogic Composition:  
 55% labradorite, optical An 65  
 20% pigeonite?  
 25% opaques
- AI-82-19 Basalt flow, bf, south of Sisters Peak
- Textures: Trachytic, possible minor glass
- Mineralogic Composition:  
 75% plagioclase, 0.4-1 mm long subhedral laths  
 3% olivine, 0.1-0.7 mm  
 10% pigeonite?, 0.05 mm  
 5% augite  
 7% opaques
- AI-82-20 Dacite from the Craigs
- Textures: Porphyritic, 1-3 mm euhedral sanidine phenocrysts composing 5% of the rock. Matrix of idiomorphic laths, 0.1-0.2 mm long
- Mineralogic Composition:  
 69% sanidine  
 5% quartz, interstitial  
 20% orthopyroxene  
 5% opaques  
 1% apatite  
 Trace allanite  
 Trace zircon
- AI-82-24 Dacite, Mountain Red Hill flow
- Textures: Porphyritic, 5 mm euhedral K-feldspar and plagioclase phenocrysts composing 1% of the rock. Matrix is subtrachytic, hypocrySTALLINE, with ragged 0.2 mm feldspar laths, cryptocrystalline mafic minerals.
- Rock contains about 10% opaques.
- AI-82-25 Dacite, Cross Hill
- Textures: Porphyritic, 1 mm K-feldspar phenocrysts compose 10% of the rock. Matrix appears about half recrystallized with interstitial quartz and albite. Mafic and opaque minerals are about 20%.

- AI-82-26                      Basalt, Two Boats basalt flow
- Textures:                      Porphyritic, 0.5 mm anhedral plagioclase phenocrysts  
compose 1% of the rock. Matrix is xenomorphic.
- Mineralogic Composition:  
59% plagioclase  
25% pigeonite and possibly augite  
15% opaques  
1% allanite
- AI-82-27                      Basalt flow, bf<sub>2</sub> vent area southwest of Lady Hill.
- Textures:                      Vesicular, hyalophitic, 0.1 mm plagioclase laths, non-  
porphyritic
- Mineralogic Composition:  
40% plagioclase  
20% pyroxene  
15% opaques  
25% glass
- AI-82-28                      Basalt flow, bf<sub>1</sub> from along English Bay road
- Textures:                      Vesicular, hypidiomorphic, non-porphyritic, 0.1-0.3 mm  
crystals
- Mineralogic Composition:  
40% plagioclase, euhedral  
15% augite and pigeonite, anhedral  
20% opaques  
25% glass
- AI-82-29                      Dacite, from the Craigs
- Textures:                      Hiatal porphyritic, 1-3 mm euhedral orthoclase  
phenocrysts compose 5% of the rock. Matrix texture is  
idiomorphic with 0.1 to 0.2 mm feldspar laths.
- Mineralogic Composition:  
70% orthoclase  
20% orthopyroxene, anhedral  
5% quartz, interstitial  
5% opaques  
Trace apatite (?)  
Trace allanite

- AI-82-32 Basalt flow, bf<sub>1</sub> vent area, South Gannet Hill
- Textures: Vesicular, few 2 mm euhedral labradorite phenocrysts. Matrix is xenomorphic with 0.3 mm crystals.
- Mineralogic Composition:  
 40% labradorite, optical An 60 on phenocrysts and An 55 on matrix crystals  
 15% pigeonite  
 25% opaques  
 1% allanite  
 20% glass
- AI-82-40 Trachitic pumice lapilli, partly welded, Green Mountain
- Textures: Compressed vitric pumice lapilli. Glass with a trace of 2 mm feldspar crystals, and small basaltic ash fragments
- AI-82-42 Basalt flow, vent area south of Spoon Crater
- Textures: Porphyritic, 1% 2-4 mm labradorite phenocrysts, trace of augite phenocrysts. Matrix is hyalophitic with 0.1-0.3 mm crystals
- Mineralogic Composition:  
 25% labradorite, optical An 62  
 7% pigeonite?, anhedral  
 68% opaque glass
- AS-2 Rhyolitic obsidian from Middleton Ridge flow
- Textures: Flow banded trachytic, with abundant elongate microlites or minute vesicles in glass
- Mineralogic Composition:  
 25% cryptolithes  
 Trace opaques  
 75% glass, clear
- AS-3 Trachyte(?), Green Mountain dome
- Textures: Holocrystalline, hiatal porphyritic with 4 mm euhedral sanadine composing 2% of the rock. 10% opaques, 0.05 to 0.01 mm. Matrix is a ragged, felsitic intergrowth partially altered to clay.

AS-5 Trachyte(?), Ragged Hill dome

Textures: Hiatal porphyritic, 3 mm euhedral microcline phenocrysts composing 20% of the rock. Matrix is 0.1-0.2 mm feldspar laths.

Mineralogic Composition:

78% feldspars, probably K-feldspar  
2% quartz, interstitial  
5% hornblende?  
15% opaques  
Trace pyroxene phenocrysts

AS-6 Andesite(?) flow, bf<sub>1</sub> south of Hummock Point

Textures: Vesicular, non-porphyritic

Mineralogic Composition:

25% plagioclase, 0.1 mm subhedral crystals  
5% pyroxene  
70% black glass  
Trace calcite in vesicles

AS-8 Trachyte(?) flow, south of Northeast Bay

Textures: Hiatal porphyritic, 1-1.5 mm microcline and andesine phenocrysts compose 3% of the rock. Matrix consists of 0.1-0.2 mm feldspar laths with small irregular vesicles and a few cumuloxyritic plagioclase and olivine xenocrysts.

Mineralogic Composition:

Most matrix minerals too small for composition estimates.  
Plagioclase about An 30.  
30% glass  
7% opaques  
Trace augite

AS-9 Andesite lava flow, north side of Green Mountain.

Textures: Vesicular, 1% phenocrysts of 2 mm anhedral oligoclase (An 25) and pyroxene.

Mineralogic Composition:

Microlites and glass with about 10% opaques  
A few amygdules of zeolites (stilbite?) are present.

- AS-10 Basalt flow, porphyritic unit south of Bears Back
- Textures: Porphyritic, 2-10 mm subhedral labradorite phenocrysts compose 25% of the rock. Matrix crystals average 0.1 mm and it has a diktytaxitic texture
- Mineralogic Composition:  
64% labradorite, optical An 55  
20% pigeonite and augite  
15% opaques  
1% allanite
- AS-11 Dacite flow, cliff unit on west end of Green Mountain
- Textures: Porphyritic, 2 mm anhedral phenocrysts of quartz and a few orthoclase phenocrysts composing 3% of the rock.
- Mineralogic Composition:  
Matrix is a microcrystalline intergrowth of secondary (?) alteration minerals, probably albite, quartz and clays. The rock is about 7% opaques
- AS-12 Bioclastic paleobeach sand, English Bay
- Textures: Well sorted fine sand, subround to subangular, weakly cemented
- Mineralogic Composition:  
84% aragonite shell and coral grains  
7% volcanic rock grains  
7% calcite cement